Cooling System Design for a Fully Superconducting Machine Used in Future Aircrafts

A Thesis

Presented to

The Faculty of the Department of Mechanical Engineering

University of Houston

In Partial Fulfillment

Of the Requirement for the Degree

Master of Science

In Mechanical Engineering

By

Pejman Bidad

December 2015

Cooling System Design for a Fully Superconducting Machine Used in Future Aircrafts

Pejman Bidad

Approved:

Chair of the Committee
Philippe Masson, Assistant Professor,
Mechanical Engineering

Committee Members:

Haleh Ardebili, Assistant Professor
Mechanical Engineering

Michael Nikolaou, Professor
Chemical and Biomolecular Engineering

Suresh K. Khator, Associate Dean,
Cullen College of Engineering

Pradeep Sharma, Professor and Chair,
Mechanical Engineering

Acknowledgment

Firstly, I would like to express my sincere gratitude to my advisor Dr. Philippe Masson for the continuous support of my M.Sc. study and related research, for his patience, motivation, and immense knowledge. His guidance helped me in all the time of research and writing of this thesis. I could not have imagined having a better advisor and mentor for my M.Sc. study.

Besides my advisor, I would like to thank the rest of my thesis committee: Dr. Robert Provence, Dr. Haleh Ardebili and Dr. Michael Nikolaou for their insightful comments and encouragement, but also for the questions which incented me to widen my research from various perspectives.

I thank my fellow lab mates for the stimulating discussions, for the days we were working together before deadlines, and for all the fun we have had.

Last but not the least, I would like to thank my family: my parents, my sisters (Salma and Najva) and also my dear cousin (Ehsan) for supporting me spiritually throughout writing this thesis and my life in general. If they had not supported me, I probably would have more problems accomplishing my higher education levels.

Cooling System Design for a Fully Superconducting Machine Used in Future Aircrafts

An Abstract

of a

A thesis

Presented to

The Faculty of the Department of Mechanical Engineering

University of Houston

In Partial Fulfillment

Of the Requirements for the Degree

Master of Science

In Mechanical Engineering

By

Pejman Bidad

December 2015

Abstract

Considering developments in superconducting machines (motors and generators), modern methods and innovations required for optimization in this field like any other energy-based systems. Meanwhile, some improvements in superconducting technologies has been drawn to flying sciences such as future turbo-electric aircrafts. Thus, companies and pioneers in this industry like NASA have been investing many resources on the aim of future aircrafts working based upon Turboelectric distributed propulsion (TeDP), Hybrid and/or electric propulsion systems. Based on the fact that superconducting machines could make gigantic saves in energy waste, they came into spotlight. This promising technology also requires demanding attentions in the area of ahead obstacles such as novel cooling methods; there have been some analyzes in this area, though. Regarding to this issue, this study is aimed to design cooling systems for superconducting machines working with liquid hydrogen (LH_2) as coolant. The indirect cooling system, which is based on both convection and conduction, has been employed. Having all sort of designs and ideas, a meander and helical shape design is recommended for rotor and stator, respectively. The results should comprise two important goals: 1) providing cryogenic temperature for system 2) evaluating pressure and outlet phase of LH_2 working in a loop. Hence, different conventional materials in cryogenic sciences have been analyzed and compared to the famous metallic mate like aluminum.

Table of Contents

List of Figures

List of Tables

1 Introduction and literature review

1.1 Background

Achieving a sustainable methods of using modern technologies without environmental damage alongside fuel-efficiency manner has been drawn to transportation services like flying systems. Meanwhile, modern air propulsion systems like turbo-electric propulsion systems are of new importance to be developed and optimized based on current needs. Superconducting rotating machines (motors and generators) are important enabling the goal of designing system optimized and more efficient. On-conventional aircrafts employing superconducting electric propulsion must analyzed and use more assessments processes to achieve this aim. However, revolutionary aircraft using superconducting machines need new designs and innovations of cry cooling technologies (based on greater power densities need) to fulfill the dream to be employed in future air industry and flying aircrafts.

One of the most important economic issues debated in recent years is determining optimized solutions for producing, transmitting and distributing Energies in aircrafts. There are several studies have been performed till today around this matter [1], [2]. Due to the lack of sufficient natural gas or other energy resources, electrical energy is the main available energy source word wide. The Subsonic Fixed Wing Project of NASA's Fundamental Aeronautics Program is researching aircraft propulsion technologies that will lower noise, emissions, and fuel burn. As already mentioned above, one promising technology is electric propulsion, which could be either hybrid electric propulsion or turboelectric propulsion. In hybrid electric propulsion, the fan would be driven with either

a turbine engine or an electric motor. In turboelectric propulsion, the turbine engine and fan would be separated; the engine would drive a generator, and the electric motor would directly drive the fan. This would allow the fans to be distributed in a way that would decrease aircraft noise. Reducing the dependence on the turbine engine would certainly reduce emissions. However, the additional weight of the electric-motor-related components that would have to be added might reduce the benefits of the smaller turbine engine. Before this technology can be implemented, research needs to be done on improving component efficiencies and reducing component weights.

In this review, some modern aircrafts have been examined, analyzed and summarized in results for being evaluated in terms of economic expenses of manufacturing process, flying duration, obstacles/benefits and also energy efficiency. These aircrafts have been selected from the most cutting-edge institutes' future projects including Glenn Research Center (NASA) [1]sophisticated plans to enhance and improve energy efficiency and also reduce and cut off waste, noise and emissions in the future flying objects [3],[4],[5].we took a look at these future goals in table (1) [6].

[1] http://www.nasa.gov/centers/glenn/home/index.html

Table 1.NASA Subsonic Fixed Wing Goals for the Next Three Aircraft Generations

Corners of trade space	N+1 (2015)***Technology Benefits Relative to a Single Aisle Reference Configuration	N+2 (2020)***Technology Benefits Relative to a Large Twin Aisle Reference Configuration	N+3 (2025)***Technology Benefits
Noise (below Stage 4)	-32 dB	-42 dB	-71 dB
LTO NOx Emission	-60 %	-75 %	Better than -75%
Performance: Aircraft Fuel Burn	-33 %	-40 %	Better than -70%
Performance: Field Length	-33 %	-50 %	Exploit metroplex* concepts

***Technology Readiness Level for key technologies = 4-6
**Additional gains may be possible through operational improvements
*Concepts that enable optimal use of runways at multiple airports within the metropolitan areas

Note that considering whether these goals can be achieved with current turbofan engines or not, might persuade us why NASA is investing on new propulsion prospects and would address this concept. Reinventing and innovation may benefit from old heat exchanger designs and materials. However, we can certainly mention that cryogenically cooled electric superconducting rotating machines (motors and generators) are classified under advanced and sort of new technologies. These machines which drive a multitude low

noise electric fans must be of great considerations to be improved. There are some examples for propulsion system as well as full aircraft of N+3 generation. High bypass ratio turbofan which is shown in figure (1), deploys a large fan mechanically connected and driven by low pressure turbines.

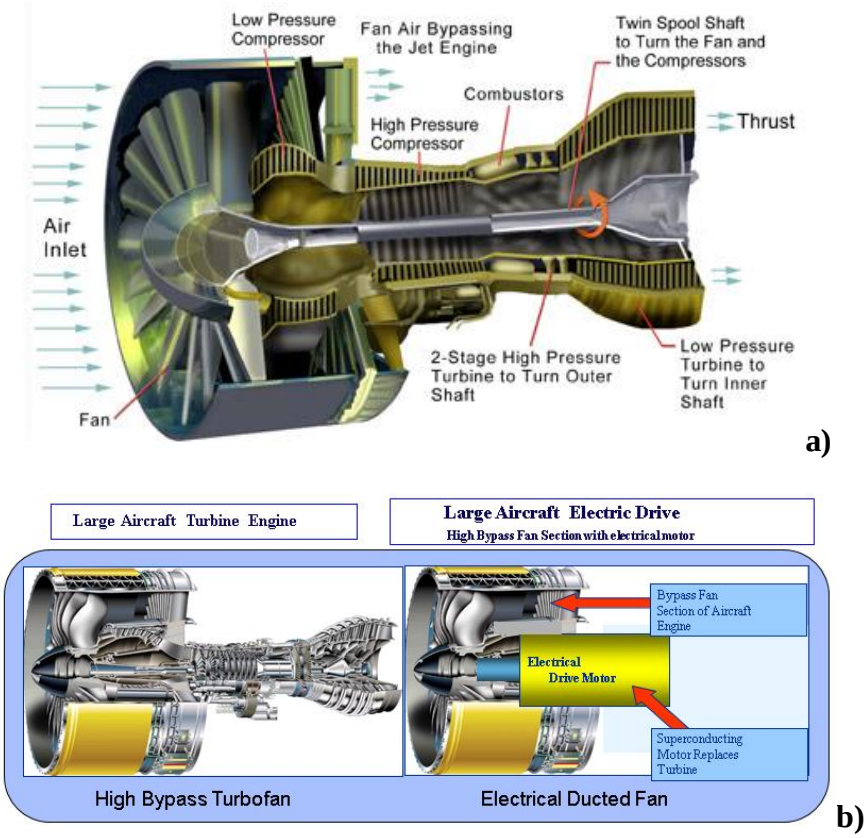

Figure 1. a) High bypass ratio turbofan b) comparison view with electrical ducted fan

The engine thrust basically is produced by the fan which itself is being rotated by the core engine. The bypass ratio (BPR) is defined as the ratio of the mass flow rate of the stream passing outside the core divided by that stream passing through the core. Generally, a higher BPR, means lower exhaust speed, which can lead to reduce fuel consumption and engine noise. The fan pressure ratio is the most important limitation needed to be

considered for any increase in BPR, however, improvements in specific power and also materials have some great results in BRP increase so far.

As can be seen in figure (1), a conventional aircraft motor worked as a coupled compressor and turbine burning fuel to produce heat energy and simultaneous rotary works of compressor and turbine make the needed thrust for these aircrafts. There are many concepts and changes have been made to improve the efficiency of these sort of propulsion systems, though, it seems the new branch of technology should be employed to design much more sophisticated propulsion systems which use less fuel burn and more reproducible and/or environmentally friendly energies. Obviously, these system make indispensable noise since air must be pressurized and jetted out to conquer against lift and drag. "In 2001, recognizing this situation, the Advisory Council for Aviation Research and Innovation in Europe (ACARE) published a 'vision' for 2020 (European Commission, 2001); this set targets of 50% reductions in fuel-burn and perceived noise, and 80% in landing/take-off NO_x emissions, relativetoyear-2000 aircraft. With both Airbus' and Boeing's plans to this date now established, it has become clear that these targets will not be achieved. They have been replaced by a new set, 'FlightPath2050' (European Commission, 2011), which calls for reductions of 75%, 65% and 90% respectively by 2050. In the U.S., similar goals have been proposed by NASA for the 'N+2' (service-entry 2025) and 'N+3' (service-entry 2030–2035) generations of aircraft (Collier, 2012)" [6].

Figure 2.CFM56–3 series turbofan engine found on the wings of the 737–300 assumptions and moving forward to TeDP/Hybrid/electric concepts

The complex challenges of meeting future environmental aims in commercial aviation require a cross-disciplinary effort that concentrates on: feasible propulsion systems, reduced fuel consumption, aviation safety and reliability, noise reduction, and optimized aircraft Design to achieve desirable flight attributes. Recent proposals for future aircraft and the convoluted challenges of meeting different demands from various aviation sectors initiate a much needed debate about the most promising aircraft propulsion systems of the 21st century. Nonetheless, there are a number of non-ignorable concepts in aviation design/manufacturing process such as distributed wheels, fuselages, landing wheels, flow control technology and propulsion technology. Similarly, it could not be ignored that propulsion systems have important ties to distribution and also energy storage systems and must be included in our studies as well [2].

The progress in commercial aviation over the last 100 years has been unparalleled. The Wright Brothers flew for 12 s over the shores of North Carolina powered by a 25 HP bicycle engine in 1903. A hundred years later, hundreds of Boeing 777 airplanes powered

by 2. GE 90 – 115 engines, fly across the globe on 8000 mile journeys. They do it repeatedly, safely, with minimum cost, low fuel consumption, low noise and low pollution. Great achievement! We, however, cannot stop there.

NASA is investigating advanced turboelectric aircraft propulsion systems that use superconducting motors to drive multiple distributed turbofans. As discussed above, conventional electric motors are too large and heavy to be practical for this application; therefore, superconducting motors are required. The major power subsystems are:

(1) Power Generation/ Conversion

(2) Energy Storage

(3) Power Management and Distribution (PMAD).

The aircraft is a hybrid electric or turboelectric aircraft means that a portion of the propulsive power comes from fuel burn: that is, this is not an all-electric aircraft. Two basic configurations exist—the hybrid electric system and the turboelectric system. **(a)** The turboelectric system converts the fuel burned to electricity via a turbo shaft engine and a generator, which provides electrical power for electric motors that drive fans to produce thrust. In this case, almost all of the thrust comes from electric motors. Figures (3) and (4) show a concept for the electrical ducted fan and a schematic of the turboelectric propulsion system, respectively. The hybrid electric system combines the turbine engine and electric motor on one shaft .Thus, propulsion comes directly from fuel and electrical power.

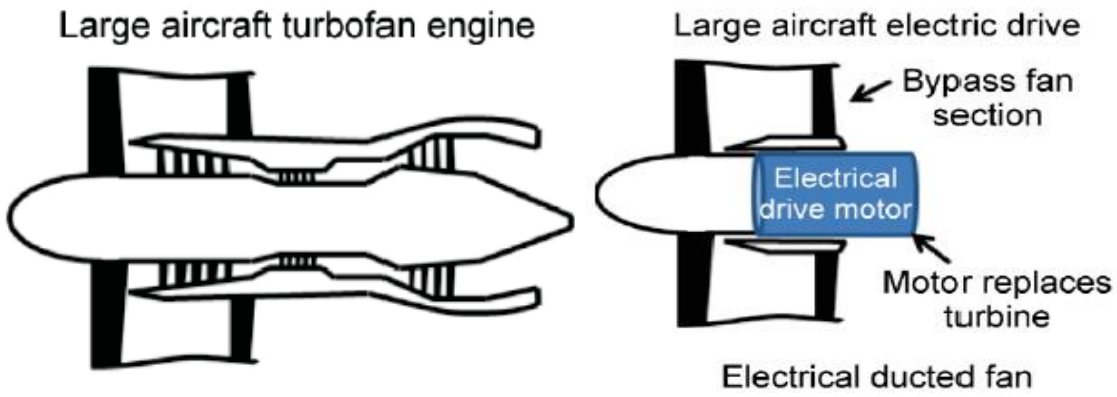

Figure 3.Comparison of turbofan and electrical ducted fan

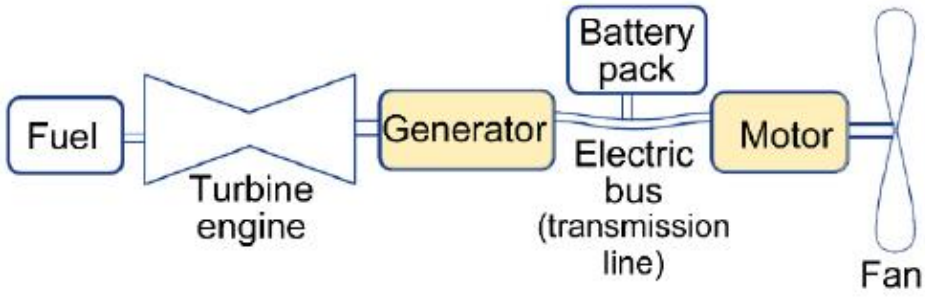

Figure 4.Turboelectric distributed propulsion system (TeDP) [9]

1.2 Cryogenics[2] and HTS[3] (High Temperature Superconductivity)

Although a chapter in this study will discuss cryogenics technologies and/or challenges, a brief introduction gathered here. The new/advanced technologies need modern methods as cooling system which classified under cryogenics sciences. the most

[2] http://en.wikipedia.org/wiki/Cryogenics
[3] http://en.wikipedia.org/wiki/High-temperature_superconductivity

important parameters for turboelectric superconducting generators which used in new TeDP systems are summarized as following: (1) Cryogenic hybrid electric aircraft will require the development of new technologies throughout the aircraft system, including superconducting motors, generators, and transmission lines; cryogenic power electronics; and cooling (e.g., cryocoolers). (2) Cryogenics is engineering design below 120 K (3) most common cryogenic fluids are liquid hydrogen and liquid Nitrogen (4) LHe is used to cool and operate superconducting magnets made with low Temp superconductors (5) LN_2 is used to cooling down system with a) intermediate shield or b) Pre cooling liquid helium magnets to 80-100 K before cooling to 4.2K [10], [11].

The aircrafts using TeDP systems need consistent cooling systems with new efficient design for the whole system. The schematic TeDP system is depicted in figures (5) and (6) also show distributed propulsion options which have been used so far.

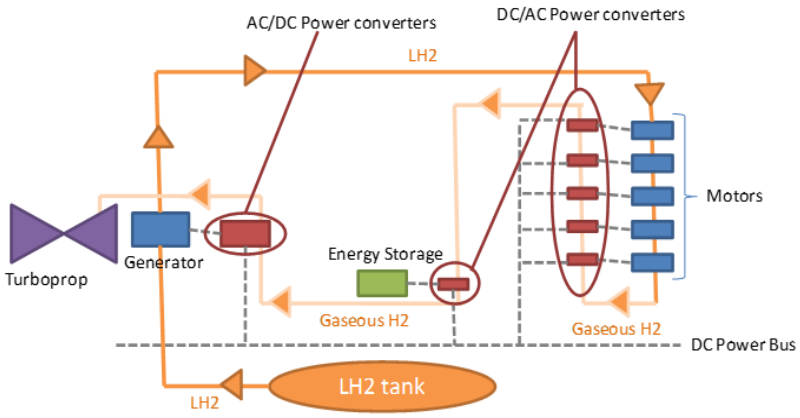

Figure 5.Turboelectric distributed propulsion system (TeDP) and cryocoolers schematic pipes

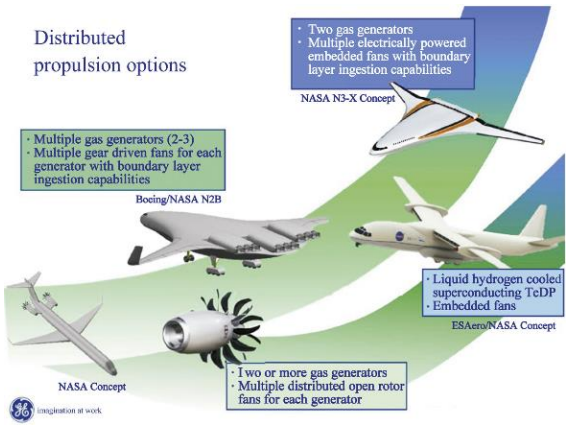

Figure 6.Distributed propulsion options [12]

Connecting multiple propulsors to a generator might be an important replacement of conventional driven functions with electronically powered components [2]. To summarize this section, we could say electric propulsion systems provide many opportunity and also challenges towards the goal of designing more efficient less emissive machines.

These challenges to design and optimize lighter superconducting machines calls new insight and attention on cooling considerations which is the majority of this study for both rotor and stator. The reason is obviously gets back to cryogenic temperature a superconducting machine can work under .Thus, there are three main prospects to be addressed:

- Cryocoolers
- Cryogen storage
- Fuels like LH2

Cryocoolers systems include cryogen which can be deployed in a close loop. The drawbacks of these systems to be mentioned, is their heavy weight for aerospace applications. The lightest cryocooler today is about 3 kg/kW input [13]. Loading sufficient cryogen as cryo-tanks at airports and/or using LH2 as onboard fuel would be some other possibilities.

1.3 Aircraft Design Based on New Propulsion Technology

Generally, fundamental changes must be made not only for designing propulsion system in modern machines but also in the design of airframe of aircraft and subsystems. Employing electric power sources such as fuel cells, modern batteries or high capacitors in a small scale or as a substitute and replacement for generators and gas turbine engines might be a good example of these changes. The problem and/or challenge for these power systems to be mentioned, is their low power/energy densities at current time. Therefore, various assessments for combination of these technologies are indispensable.

1.4 Machine configuration:

Some popular configurations for these machines are possible like: Radial flux machines or Trapped flux magnet excited machines. Basically, as the high critical current density provided by superconducting tapes in superconducting machines (motors and generators), the need of an iron core is removed and these machines have considerable reduced weight and size compared to conventional ones. With this replacement, which itself calls cooling designs to provide the cryogenic temperature, electrical losses will be reduced significantly. For particular models of designs, different material would be suggested like MgB_2, Bi2223 or YBCO conductors. The discussions and definitions of

model in this study will be gathered in simulation chapter. Although the NASA aircraft design study is continuing, a description of distributed turboelectric propulsion for hybrid wing body aircraft is gathered as following section. The resulting weights and efficiencies of each of the electrical components is presented in Table (2) for magnesium di-boride (MgB2) and in Table (3) for bismuth strontium calcium copper oxide (BSCCO) [14].

Table 2.MgB2 Based Electrical System Weights and Efficiencies.

	MgB_2		
Component	Weight (lb)	Efficiency (%)	Specific Power (hp/lb)
Generator,	1184	99.98%	25.3
Generator Cooler	1005		
Generator with Cooler	2189	99.28%	13.7
Transmission line	1000		
Inverter	200	99.93%	20
Inverter Cooler	67	99.57%	
Inverter with Cooler	267	99.50%	15
Motor	314	99.97%	13.4
Motor Cooler	202		
Motor with Cooler	516	98.95%	7.8
Total -Cryocooled	17123	**97.75%**	3.5
Total - LH2 Cooled	11078	**99.88%**	5.4

Table 3.BSCCO Based Electrical System Weights and Efficiencies.

	BSCCO		
Component	Weight (lb)	Efficiency (%)	Specific Power (hp/lb)
Generator,	954	99.93%	31.4
Generator Cooler	580		
Generator with Cooler	1534	99.55%	19.6
Transmission line	1000		
Inverter	200	99.93%	20
Inverter Cooler	67	99.57%	
Inverter with Cooler	267	99.50%	15
Motor	298	99.94%	13.4
Motor Cooler	93		
Motor with Cooler	391	99.48%	10.2
Total -Cryocooled	13938	**98.54%**	4.3
Total - LH2 Cooled	1037	**99.80%**	5.8

Also, in table (4) a comprehensive comparison of different propulsion systems for aircrafts is presented.

Table 4.compares different propulsion systems for aircrafts. [1]

Propulsion System	Components	Weight, lb (kg)	Efficiency, %	TSFC, hr–1
Turboelectric distributed fans (refrigerated)	Two 42 380 hp engine cores	7300 (3300)	-	0.57
	Two 42 380 hp electric generators (including refrigerators)	3000 (1300)	99.7	-
	Sixteen 5250-hp motors (including refrigerator)	4700 (2100)	99.4	-
	total	**15 000 (6800)**	99.1	-
Turboelectric distributed fans (LH2 cooled)	Two 42 080-hp engine cores	7300 (3300)	-	0.57
	Two 42 080-hp electric generators (LH2 cooled)	1900 (860)	99.9	-
	Sixteen 5250- hp motors (LH2 cooled)	3100 (1400)	99.9	-
	total	**12 300 (5600)**	**99.9**	-
Conventional small distributed turbofans	Sixteen 5250-hp engine cores	**10 000 (4500)**	91	**0.63**
Conventional large non-distributed turbofans	Two 42 000-hp engine cores	**8700 (4000)**	-	**0.57**

2 Cryogenics

2.1 Introduction:

Cryogenics plays a vital role in superconducting machines, however, it calls for increase in cost, complexity and instability of a system (stability is a character of a system, i.e., when a perturbation is applied to a system like superconducting machines, the system tends to be excited and instable, and once the system returns to its original state, the system would be stable). The thermal sciences and systems also need this stability, why? The answer is not tough and would imply to continuity of system operation [15].

This wide field of science is very demanding and faces with versatile challenges requiring new insights and efforts. This branch of applied science can be defined as:" a specialized branch of applied physics and engineering involving technology associated with temperatures below 120 K". This is mainly focused towards the study of low temperature and studying material behavior at low temperature. Liquefying the 'non-condensable' gases would be of attention interest hence. There would be some challenges listed below associating with cryogenics:

- Dealing with materials properties and the state of their mixtures
- Turbumachinery
- Thermal insulation technologies and methods
- Fluid flow, heat sinks design and/or CFD
- Experimental evaluation for systems prototype

Since local thermal stability of superconductors is defined and governed by various mechanisms, Cryogenics for high temperature superconductors (HTS) does not necessarily

mean operation at the temperature of liquid nitrogen or near its critical temperature. For any application, the power and current density are important since it is clearly most efficient to operate a superconductor near its highest allowed temperature. Besides, answering the question for best possible temperature for a superconducting system requires the deep knowledge on HTS and magnet systems functions, as well as their cost evaluation. A combination of engineering and scientific disciplines, assigned to realize the behavior of materials, systems and equipment's in low temperatures classified as cryogenics. The study of cryogenics will make physicists and engineers fully conversant with phase transitions, supercritical fluids, two phase flows, non-linear heat transfer regimes, flow instabilities and fields in advanced science and technology. Technically, establishing a cryogenic system faces these fields and/or challenges [16]:

- structural materials
- assembly and joining methods
- sealing operation and safety besides improving efficiency
- knowledge of risk analysis

2.2 Cryogenic liquid

Basic understanding of cryogenic liquids is necessary for understanding any applications using cryogenics as described in this chapter. The commonly used cryogenic fluids are given in Table (5) [16].

Table 5.commonly used cryogenic fluids properties

Cryogenic fluid property	He	H2	Ne	N2	Ar	O2	CH4
Molecular weight	4.00	2.02	20.18	28.01	39.95	32.00	16.04
Critical temperature (K)	5.20	33.18	44.49	126.20	150.7	154.60	190.6
Critical pressure (atm)	2.25	12.98	26.44	33.51	47.99	49.77	45.39
Boiling point (K)	4.23	20.27	27.10	77.35	87.30	90.20	111.7
Melting point (K)	4.2	13.95	24.56	63.15	83.81	54.36	90.72
Density of liquid at b.p. (kg/m3)	124.7	70.8	1207	806.1	1395	1141	422.4
Density of gas at 273 K and 1 atm (kg/m3)	0.1785	0.0899	0.8998	1.25	1.784	1.429	0.7175
Thermal conductivity of liquid at b.p. (mW/(m-K))	18.66	103.4	155	145.8	125.6	151.6	183.9
Latent heat of vaporization (*hfg*) at b.p. (kJ/kg)	20.75	445.4	85.75	199.2	161.1	213.1	510.8

Any superconducting system with superconducting magnets or associated with superconductivity demands proper understanding of the cooling technology. In order to address the issues in cryogenics following consideration must be taken:

- cooling sources(liquid cryogens or cryocooler are employed to cool down the magnets)
- Heat sources and measurement technology.

There are primarily two methods of cooling a sample for cryogenic measurement:

- **Direct Cooling:** this method uses direct immersion of the sample in a cryogenic liquid. Ideal for sample heating at high current densities regardless of shape. Cooling wet magnets using this method, allows easy and efficient cooling independent of shape because applying direct cooling enhances the high heat transfer coefficient between the cooling medium and the heat removal surface.
- **Indirect Cooling:** The second method is through an intermediate medium (basically conduction cooling) where the sample is attached to cold body cooling down by different methods available. Figure (7) shows a schematic diagram of this method.

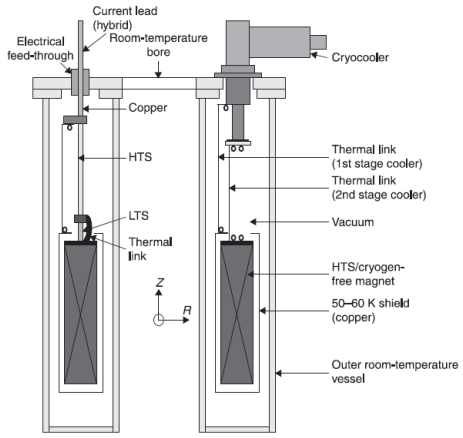

Figure 7.Schematic of conduction cooling magnet system in cryostat.

Although in this method the cooling power is limited, the methods reduces the challenges dealing with cryogenic fluids. Three commonly used fluids as coolants are:

- Liquid Hydrogen (LH2)
- Liquid helium (LHe) is used to cool and operate superconducting magnets fabricated from low temperature superconductors,
- Liquid nitrogen

Liquid nitrogen can be used for pre-cooling liquid helium magnets to 80–100K before cooling to 4.2 K. Cryogen-free (dry) and HTS magnets are currently cooled by a cryocooler, whose cold head section is attached to one end of the magnets. Assuming that we have no additional heat load except magnets, which are cooled by cryocooler as a source (in a adiabatic volume), and with these parameters: The mass of the magnet can be represented by (*m*), heat capacity (*c*), and density (ρ),our aim is to achieve the stable thermal condition which means *T magnet = T Cooler*. From the first law of thermodynamics we can write for *Q Cooler*:

$$-\mathrm{Q}_{\mathrm{cooler}} = \left(\frac{\mathrm{m}}{\rho}\right).\mathrm{C}.\frac{\mathrm{dT}}{\mathrm{dt}}, \qquad (1)$$

while the cooling progress $dT/dt < 0$ ($-$ *Q Cooler* represents the heat sink providing cooling).we could rewrite this equation as equation (2):

$$\mathrm{dt} = \left(\frac{\mathrm{m}}{\rho}\right).\mathrm{C}.\frac{\mathrm{dT}}{\mathrm{Q}_{\mathrm{cooler}}}. \qquad (2)$$

The time constant τ can be calculated by integrating Equation (3) between the operating temperature and final temperature. The time needed to cool the magnet is given as:

$$\tau = \left(\frac{m}{\rho}\right).\int_{T_{op}}^{T_{final}}\left(\frac{C}{Q_{cooler}}\right).dT = \frac{m}{\rho}\int_{T_{op}}^{T_{final}} K.dT, \quad (3)$$

where K = C / Q_{Cooler}, T_{op} is the operating temperature and T_{final} is the final temperature that needs to be achieved. Note that this equation clearly shows if there would be a balance between mass and cooling power provided, we could reduce the time.

Cryogens have great cooling power and are mostly used for direct cooling, but with cryocoolers, and their limited cooling power, the system is cooled by conduction. There are only a few cryogens that have an atmospheric saturation temperature (boiling point) below 100 K. Liquid helium is so popular for LTS/HTS superconductor magnets. Amongst the main cryogens (helium, hydrogen, neon, nitrogen and oxygen), helium is the only cryogen suitable for LTS magnets [17, 18]. For HTS magnets, it is always best to operate them dry, and not wet. If operated wet, hydrogen, neon and nitrogen all cover the operating temperature range with limitations to specific critical parameters, but safety needs close attention. Also For HTS applications, there are three solid cryogens as following:

- solid nitrogen (SN_2),
- solid neon (SNe), and
- Solid argon (SAr).

Detailed analysis of the thermodynamic and mechanical properties of the above solid cryogens suggests that SN_2 is the preferred candidate for cooling HTS. SN_2 remains solid up to 64 K with good electrical insulation properties and is inexpensive, which makes

it preferable. Hence, for HTS magnets operating at a temperature in 20–60 K using BSCCO or YBCO and MgB_2 operating in the range 10–30 K, SN_2 gives an enhanced thermal capacity and acts as a thermal reservoir. In general, solid cryogens have good heat capacity and are a substitute for impregnants. Solid cryogens are preferred over epoxy in certain applications for the following reasons: thermal conductivity, mechanical strength and electrical insulation [19].

2.3 Cooling methods

There have been several important cooling methods as following:

- Bath-cooled cryostat: coolant in direct cooling (heat transfer is both conduction and convection),
- Forced cooled: coolant is forced to flow under pressure inside the coil winding as an in cable in conduit conductor (heat transfer is both conduction and convection),
- Cryocooled: The system is cooled using cryocoolers (heat transfer is conduction).

A block diagram of a typical cryogenic refrigerator is shown in Figure (8) [20]:

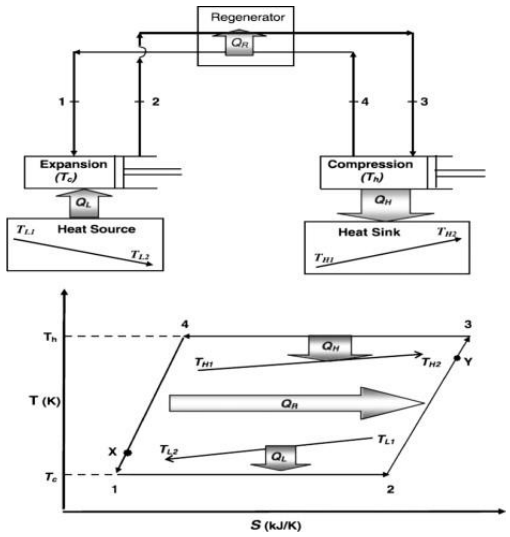

Figure 8.block diagram of a typical cryogenic refrigerator

The HTS device needs to operate at cold temperature (Tc heat source). The source of this heat load would be radiation, solid/gas conduction and fluid convection from adjacent regions or body structures at higher temperatures. The heat from the source must be transmitted to the cold region of the refrigerator by 1) solid conduction or 2) fluid convection. Indeed, this causes the temperature gradient between two regions. The working fluid(which is Liquid hydrogen in this study and will be discussed more in the next sections) in the cold part absorbs heat and flows next to a heat exchanger where this fluid is further heated by exchange with a counter-flow gas stream. Then, based on pressure drop, it should be transferred to a compressor where external work is done on the fluid, compressing it to high pressures and further increasing the fluid temperature. Thereafter, this fluid flows to an environment heat exchanger/sink where the heat of compression is rejected to the ambient near room temperature (at T_h). Next the fluid goes to the heat exchanger mentioned above where it is further cooled by rejecting heat to the counter-flow gas stream or regenerative matrix. From here the cold fluid can go to the load or be further cooled by expansion of the fluid to remove heat. The efficiency of an ideal process (called the coefficient of performance, COP) for such a refrigerator can be shown as:

$$\eta_{carnot} = \frac{T_C}{T_h - T_c}, \tag{4}$$

where η_{carnot}= Carnot efficiency, T_h= higher operating temperature (ambient), T_C = lower operating temperature. Several observations can be made. T_C in HTS applications is in the range 25–80 K compared to 4–10 K typical of LTSs. However, Real refrigerators typically

run at a fraction (less than 10% and up to 30%) of Carnot efficiency due to losses in compressors, heat exchanger effectiveness, etc.

Typically, the heat load to the system is usually measured based on pressure, temperature and mass flow rate of input and output. In most cryogenics systems, heat loads have been measured on large-scale systems, mostly to cover the issues surrounding the accuracy of measurement. For a large system, the heat-load balance including the cryogenic is given by Equations (5) and (6) as following [21]:

$$Q_{total} = Q_{HTS,system} + Q_{Cryogenics} = \dot{m}(h_1 - h_2) = \dot{m}c_p(T_1 - T_2) \text{ and} \quad (5)$$

$$Q_{HTS,system} = \left(Q_{conduction} + Q_{radiation} + Q_{joul-heating}\right)_{CL\_Bus} + Q_{crtostat} + Q_{HTS}. \quad (6)$$

2.4 Cryostat design

Based on the versatile applications, limitations (space, cost...) and challenges, every cryostat might be designed. However, some of these parameters which narrow the design will be listed as following:

- Operating condition such as cooling power needed and temperature range
- Available and/or attainable equipment like pumps
- Magnetic specifications and requirements
- Ease of access and system maintenance
- Mechanical coupled thermal design

2.5 Conduction heat transfer: solid, liquid and gases

Heat conduction (or thermal conduction) is the movement of heat from one solid to another one that has different temperature when they are touching each other. For example, we can warm our hands by touching hot-water bottles. When the cold hands touch the hot-water bottle, heat flows from the hotter object (hot-water bottle) to the colder one (hand). Other ways to transfer heat are by thermal radiation and/or convection. Usually more than one of these processes happen at the same time. Conduction is the most significant means of heat transfer within a solid and between solid objects in thermal contact. Fluids are less conductive, with the exception of helium. Therefore the thermal contact conductance between solid bodies in contact is vital for cryogenic design and applications that need to cool the system with cryocoolers. There are two main states under which conduction act:

- Steady state conduction
- Transition conduction

There is one important concept as "steady state condition", assigned when the amount of heat entering a system is equal to the amount of heat removed. On the other hand, Transient conduction occurs when or where the temperature changes with time. Conduction loss is normally calculated using Fourier's law as given in equation (7) [22]:

$$\frac{\partial Q}{\partial t} = -k \oint_S \nabla T . dS, \tag{7}$$

where Q is the amount of heat transferred, t is the time taken, k is the material's thermal conductivity, S is the area through which the heat is flowing, and T is the temperature. Heat conduction through gases is normally used for cooling samples (as exchange gas) and/or for shielding (vapor cooling). The heat transfer rate between the solid and gas having

a temperature gradient (ΔT) is expressed by Newton's law of cooling (Eq. 8) [21], where the rate of heat transfer is proportional to the difference in temperatures between the body with its surroundings and heat transfer co-efficient:

$$\dot{q}_{Convection} = h_{Convection} . A_{Surface} . \Delta T, \quad (8)$$

where $h_{Convection}$, is the convective heat transfer coefficient and *A Surface* is the surface area of the solid. The heat transfer under forced convection is much greater than the free convection, which is mostly proportional to the density gradient of material. Also, the convective heat transfer would be much larger as the velocity increases, like conditions pumps or fans employed to flow the fluid faster.

2.6 Radiation heat transfer

In physics, radiation is the emission or transmission of energy in the form of waves or particles through space or through a material medium. Heat transfer through radiation takes place in form of electromagnetic waves mainly in the infrared region. Radiation emitted by a body is a consequence of thermal agitation of its composing molecules, represented by the Stefan–Boltzmann equation as following [21]:

$$\dot{q}_{Radiation} = \sigma . \varepsilon . A . (T_{hot}^4 - T_{cold}^4), \quad (9)$$

where ε is the emissivity of the surface at operating temperature, *A* is the surface area of the incident heat flux, and σ is the Stefan–Boltzmann constant ($5.67 \times 10 -8$ W/m ^{2} .K ^{4}). In order to reduce the radiation heat flow ε a temperature gradient is introduced using an additional 'line of sight' shield (sometimes referred to as a radiation shield). Multiple radiation shields break the temperature gradient into smaller steps thereby significantly

reducing radiation heat transfer into the low temperature surfaces. In principle, with N floating (rigid to semi-rigid) radiation shields, the radiation heat transfer could be reduced by $15 \sim (N+1) - 1$ [21].

2.7 Joule heating due to transport current

There are more heat sources that are important for a cryostat design for both wet and dry systems that significantly affect the thermal design and performance. Resistive heating, also referred to as joule heating, is experienced primarily from (a) the sample contacts, which can be minimized by good sample cooling and making low-resistance sample contacts and (b) current leads – this is normally optimized based on the operating cycle, cross-section area, cooling power available and protection for the lead itself [19].

2.8 Material selection

The most important limitations narrow our efforts in designing cryostat structure related to material properties. This affair sensed better in choosing materials used in contact and/or at specific unpopular operating conditions. The following properties are critical to be considered: 1) thermal, 2) mechanical and 3) electrical design (structural, support, cooling, etc.). Well-known example for expanding this issue is the difference thermal conductivity of metals and ceramics, where favorable sample holder at heat sinks built from metals like copper instead of ceramics, whereas at first glance ceramics have much greater thermal conductivity [23].

2.8.1 Thermal properties

Thermal conductivity is the most significant parameter for the purpose of cryogenics in superconducting machines, and also will open a broad way of demanding

efforts and challenges. The materials most widely used in cryogenics are copper, brass, stainless steel, glass, epoxy composites, Kapton™ and Teflon™ of various grades and ceramics. Higher purity metals will have higher thermal conductivity at cryogenic temperatures. The options are limited at present to using sapphire and/or beryllium oxide (beryllia) as a medium to isolate electrically from the cooler stage/heat sink. Although, austenitic stainless steel is classified as Low-thermal-conductivity components in the cryostat (usually for cryostat structure), they are of high strength properties. Once there is a need for some materials with high strength and low thermal/electrical conductivity, non-metallic materials might be used. To name some, fiber glass–epoxy composites (G10), Kapton™, Mylar™ and resins filled with glass, cloth or paper (Tufnol™) have to be mentioned.

2.8.2 Heat capacity:

This normally is classified in terms of specific heat, a measure of the amount of heat that can be removed by lowering the temperature by 1 K. In general heat capacity decreases substantially at cryogenic temperatures to about T^3 (lower operating temperature). Therefore at cryogenic temperatures some systems take longer to cool down and stabilize (thermal equilibrium) than others. Ceramics and epoxy/resin-filled composites have higher specific heat capacities of about an order of magnitude more than metals over the same range of temperature [24].

2.8.3 Mechanical properties

This is the prime concern for structural materials, and we do not use materials that embrittle on cooling. Hence this limits the use of most iron alloys such as carbon steel and Fe-Ni steels that are very good at room temperature. As discussed briefly above, FCC-

structured materials such as copper, aluminum; brass and austenitic steel are used due to their excellent ductile properties at cryogenic temperatures. With careful design on thermal stress and strain, titanium hexagonal closed pack (HCP) and niobium for shielding body-centered cubic (BCC) can also be used. While designing the structural materials for room and cryogenic temperatures, the yield strength is considered at the operating temperature, along with its magnetic susceptibility properties [19].

2.8.4 Magnetic properties (magnetic susceptibility)

Magnetic properties is another important factor needed to be studied and evaluated before any design of superconducting machines. We will more discuss about them in the following chapters.

3 Turbulent Flow

For modeling every phenomenon, we should first have a deep knowledge of them. We are dealing with turbulent flows as the most popular flows exist in the nature such as channels flows, air conditioning systems flows, wind, gas pipes etc.

We could state this as: "*turbulent flow is basic and laminar one is an exception.*"

For laminar flow we need low scale geometries and also high viscosity flows. Each turbulent flow has both vortex and perturbation structures inside. For a turbulent flow we have some common specifications:

- **Irregularity and randomness:** is a common characteristic for all turbulent flows. For such this matter, applying statistical methods are popular among researchers nowadays.
- **Diffusivity:** is defined as transport by eddies instead of molecules. To be clear, in laminar flows we have molecular transport rather than eddies.
- Turbulent flows have high **Reynolds number**
- Turbulent flows have **rotational movement,** and consequently this causes fluctuating vortices. Turbulence has a complex structure and include a vast spectrum of eddies.
- **Dissipation:** Turbulent flows consume energies! It means they need energy to keep their characteristics as turbulence flow.
- Turbulence is a character of flow not fluid, so the model which is defined by turbulent theory is valid for both liquids and gases.

- Perturbations in turbulent flows are of important intrinsic specifications defined by their fluctuation rate.

3.1 Molecular Diffusion[4]:

Caused by movements of molecules of a fluid in accordance to heat energy available. In kinetic theory of gasses, assumptions are based on the fact that each molecule moves in a direct path with a constant velocity. These molecules impact to each other, consequently, the direction and magnitude of velocity change. The mean distance a molecule passes before the next impact to the next molecule is called 'mean free path'.

The Molecular Diffusion eventually leads to a uniform density of a mixture or material all around its texture.

3.2 Turbulent Models:

After time averaging of terms in Momentum equations, some term appeared which Reynolds called them Stresses. Since there is no direct method to calculate these terms, they must be modeled based on known quantities such as mean velocity of flow. Generally, turbulent models are some coupled equations which are able to calculate Reynolds stresses that could be consistent with experimental and empirical results. There are different well-known turbulent models introduced so far.

In another classification, turbulent models divided into two categories:

- Models which use eddy viscous [25]

[4] **Diffusivity** or **diffusion coefficient** is a proportionality constant between the molar flux due to molecular diffusion and the gradient in the concentration of the species (or the driving force for diffusion). Diffusivity is encountered in Fick's law and numerous other equations of physical chemistry.

- Models which obtain Reynolds Stresses directly from equations.

3.3 The equation which use eddy viscous concepts are:

- Zero equation Models: the simplest form of turbulence models defined by Prandtl [5]in 1925
- One equation Models: Introduced to compensate the deficiency in Zero equation models which could not be able to consider transport terms.
- Two equation Models: while One equation Models give better results compared to Zero equation Models ,especially for simulating flows in pipes, they still cannot consider transport effect on the mixture length. This length also is an empirical amount in One equation Models. So L_m or mixture length is being obtained by a separate transport equation in these sort of models.

3.4 Reynolds stress [6]Model (RSM):

This model is the most general and direct models to simulate Turbulence. RSM models employ mathematical operations to obtain Reynolds Stresses directly from equations.

3.5 Approach to other turbulence models:

In any turbulent problem, the swirling flow would be of important attention. Let's first define swirling number.

[5] Ludwig Prandtl (4 February 1875 – 15 August 1953) was a German engineer. He was a pioneer in the development of rigorous systematic mathematical analyses which he used for underlying the science of aerodynamics, which have come to form the basis of the applied science of aeronautical engineering. In the 1920s he developed the mathematical basis for the fundamental principles of subsonic aerodynamics in particular; and in general up to and including transonic velocities. His studies identified the boundary layer, thin-airfoils, and lifting-line theories. The Prandtl number was named after him.

[6] In fluid dynamics, the **Reynolds stress** is the component of the total stress tensor in a fluid obtained from the averaging operation over the Navier-Stokes equations to account for turbulent fluctuations in fluid momentum.

3.5.1 Swirl Number:

Swirl number based upon what has been discussed so far is the main key in turbulence and swirl behavior in cyclonic flows. The swirl number is defined by equation (10):

$$S = \frac{G_\phi}{G_x \times R}, \qquad (10)$$

where G_Θ is the angular momentum and G_x is the axial momentum. R is the radius of cyclone or any cyclonic flow regime. So, equations (11-a) and (11-b) give another forms of equation (10) as below:

$$G_\phi = \int_0^R \rho 2\pi r u dr \times r\omega \text{ and} \qquad (11\text{-a})$$

$$G_x = \int_0^R 2\pi r \rho u dr \times u + \int_0^R p 2\pi r dr . \qquad (11\text{-b})$$

The swirl number can be changed in simulation, but the common chosen number is 0.6-0.7 in simulation modeling. As we have seen, the mathematical models have some problems. One very important problem is that they usually:

1. Consider flow as a fully developed region
2. Ignore important parts in momentum equations to simplify the equations

The goal of mathematical method is to solve the continuity and momentum equations analytically, but unfortunately, they need to simplify more equations to obtain

simple ones to be solved. So in complicated modeling and/or in that situation we need real condition of flow with higher accuracy those kind of mathematical modeling will not be of importance compared to other solutions and techniques CFD and simulation programs use.

3.6 Popular Turbulence Models:

We can divide turbulence models into five main categories which basically used in solving applications and softwares (finite-element-based softwares):

- k-ε standard
- RNG k-ε
- k-ε Realizable
- Spalart-Allmaras (S-A)
- RSM

3.7 Introduction to Modeling:

For an incompressible fluid flow, the equation for continuity and balance of momentum are given as equation (12) [26]:

$$\frac{\partial \overline{u_i}}{\partial x_i} = 0,$$

$$\frac{\partial \bar{u}_i}{\partial t} + \bar{u}_j \frac{\partial \bar{u}_i}{\partial x_j} = -\frac{\frac{1}{\rho}\partial \bar{P}}{\partial x_i} + \nu \frac{\partial^2 \bar{u}_i}{\partial x_j \partial x_j} - \frac{\partial}{\partial x_j} R_{ij}.$$

$$\frac{\partial}{\partial t} R_{ij} + \overline{u_k} \frac{\partial}{\partial x_k} R_{ij} = \frac{\partial}{\partial x_k}\left(\frac{\nu_t}{\sigma^k} \frac{\partial}{\partial x_k} R_{ij}\right) - \left[\frac{R_{ik}\frac{\partial \overline{u_j}}{\partial x_k} + R_{jk}\partial \overline{u_i}}{\partial x_k}\right]$$

$$-C_1 \frac{\varepsilon}{K} R_{ij} - \frac{2}{3}\delta_{ij} K - C_2 \left[P_{ij} - \frac{2}{3}\delta_{ij} P\right] - \frac{2}{3}\delta_{ij}\varepsilon. \quad , \qquad (12)$$

where the turbulence production terms P_{ij} are defined as equation (13) [26]:

$$P_{ij} = -\left[R_{ik}\frac{\partial \overline{u_j}}{\partial x_k} + R_{jk}\frac{\partial \overline{u_i}}{\partial x_k}\right], P = \frac{1}{2}P_{ij}. \tag{13}$$

The transport equation for the turbulence dissipation rate 'ε' is given as below [27]:

$$\frac{\partial \varepsilon}{\partial t} + \overline{u_j}\frac{\partial \varepsilon}{\partial x_j} = \frac{\partial}{\partial x_j}\left[\left(\nu + \frac{\nu_t}{\sigma^{\varepsilon}}\right)\frac{\partial \varepsilon}{\partial x_j}\right] - C^{\varepsilon 1}\frac{\varepsilon}{K}R_{ij}\frac{\partial \overline{u_i}}{\partial x_j} - C^{\varepsilon 2}\frac{\varepsilon^2}{K}. \tag{14}$$

As previously discussed, since turbulent flows have a different temporary value for variables besides an average one, the momentum equation for one direction is given as equation (15):

$$\frac{\partial(u+u')}{\partial t} + u\frac{\partial(u+u')}{\partial x} + v\frac{\partial(u+u')}{\partial y} + \omega\frac{\partial(u+u')}{\partial z} = \frac{-1}{\rho}\frac{\partial(p+p')}{\partial x} + \upsilon\nabla^2(u+u'). \tag{15}$$

For this equation after simplifying process, we have a simple form like equation (16):

$$\frac{Du}{Dt} + \frac{\partial u'}{\partial t} + u\frac{\partial u'}{\partial x} + u'\frac{\partial u}{\partial x} + u'\frac{\partial u'}{\partial x} + v\frac{\partial u'}{\partial y} + v'\frac{\partial u}{\partial y} + v'\frac{\partial u'}{\partial y} + \omega\frac{\partial u'}{\partial z} + \omega'\frac{\partial u}{\partial z} + \omega'\frac{\partial u'}{\partial z} = \frac{-1}{\rho}\frac{\partial p}{\partial x}\frac{-1}{\rho}\frac{\partial p'}{\partial x} + \upsilon\nabla^2 u + \upsilon\nabla^2 u'. \tag{16}$$

This equation has many terms but we can even simplify it by adding this three terms to the LHS, because the summation of these three terms based on Continuity equation is zero. These term are given in equations (16-a), (16-b) and (16-c):

$$u'\frac{\partial u'}{\partial x}, \tag{16-a}$$

$$u'\frac{\partial v'}{\partial y}\text{, and} \tag{16-b}$$

$$u'\frac{\partial \omega'}{\partial z}\text{.} \tag{16-c}$$

Finally, we have the simplified equation (17) as given:

$$\frac{Du}{Dt}+\frac{\partial \overline{u'^2}}{\partial x}+\frac{\partial \overline{u'v'}}{\partial y}+u'\frac{\partial \overline{u'v'}}{\partial z}=\frac{-1}{\rho}\frac{\partial \bar{p}}{\partial x}+\upsilon\nabla^2 u\,. \tag{17}$$

Cleary, equation (17) has some unknown terms. These are based on Reynolds Theorem, called Reynolds stresses. Actually, the main difference between Navier-Stocks equations and Reynolds equations is the existence of these three terms. The whole number of these terms are nine, as a tensor, but six of them are equal and three are unique, the shear stresses and normal stresses, respectively. Finding these quantities is one of the main differences between turbulence models.

3.8 Zero equation Model (Prandtl) [28]:

As we know previously, we have laminar viscosity which has been defined by this equation:

$$\tau=\frac{F}{A}=\mu\frac{\partial u}{\partial y}, \tag{18}$$

where, F is force, A is area, and u is velocity.

In turbulent flows we have another viscosity defined based on eddy viscosity concept [25].

3.9 Boussinesq Model:

Boussinesq [7][29-30] introduced the famous equation (19) as given below:

$$-\rho\overline{u_i'u_j'} = \mu_t\left(\frac{\partial u_i}{\partial x_j} + \frac{\partial uj}{\partial xi}\right) - \frac{2}{3}\rho k\delta_{ij}, \tag{19}$$

where kronecker[8] delta is either zero or one. Based on this equation different researches have been carried out to give a method to find out μ_t as the eddy viscosity. Prandtl defined a new equation as equation (20):

$$\mu_t = \rho\ell_m^2\left|\frac{\partial u}{\partial y}\right|, \tag{20}$$

where, l_m is the mixing length here. So other models such as one equation model or two equation models have been introduced to cover the weaknesses and deficiencies of mathematical malfunctions. There are approximations for this equations based on even experimental work.

3.10 K-Epsilon equations:

There are three branches of K-Epsilon models: RNG, standard and finally realizable. These models recommended that are not the optimized ones to be employed in one particular problem [31]. K and epsilon have been formulated as equations (21-a) and (21-b):

[7] **Boussinesq approximation** may refer to several modelling concepts – as introduced by Joseph Valentin Boussinesq (1842–1929), a French mathematician and physicist known for advances in fluid dynamics

[8] **Leopold Kronecker** (7 December 1823 – 29 December 1891) was a German mathematician who worked on number theory and algebra. He criticized Cantor's work on set theory, and was quoted by Weber (1893) as having said, "*Die ganzen Zahlen hat der liebe Gott gemacht, alles andere ist Menschenwerk*" ("God made the integers, all else is the work of man.")

$$\frac{\partial}{\partial t}(\rho K)+\frac{\partial}{\partial x_j}\left(\rho u_j K\right)=\frac{\partial}{\partial x_j}\left(\frac{\mu_t}{\sigma_k}\frac{\partial K}{\partial x_j}\right)+G_k-\rho\varepsilon \quad \text{and} \qquad (21\text{-a})$$

$$\mu_t=\rho K^{1/2}\ell_m . \qquad (21\text{-b})$$

Also, for Epsilon we have these four equations as given in equation (22-a) to (22-d):

$$\varepsilon=C_\mu\frac{k^{3/2}}{l_m}, \qquad (22\text{-a})$$

$$F_D=C_D\rho l_m^2\left(k^{1/2}\right)^2\rightarrow P_D=\frac{k^{1/2}\times F_D}{\rho l_m^3}=\frac{C_D k^{3/2}}{l_m}, \qquad (22\text{-b})$$

$$\frac{\partial}{\partial t}(\rho\varepsilon)+\frac{\partial}{\partial x_j}\left(\rho u_j\varepsilon\right)=\frac{\partial}{\partial x_j}\left(\frac{\mu_t}{\sigma_\varepsilon}\frac{\partial\varepsilon}{\partial x_j}\right)+C_1\frac{\varepsilon}{K}G_k-C_2\rho\frac{\varepsilon^2}{K} \text{, and} \qquad (22\text{-c})$$

$$\mu_t=\rho C_\mu\frac{K^2}{\varepsilon} . \qquad (22\text{-d})$$

Solving these equations need softwares and applications which are known by simulation or modeling ones. The reason is the complexity of simultaneous solution which takes a long time of process.

3.11 RSM model:

The main equations is given as equation (23):

$$\frac{D\overline{u_i'u_j'}}{Dt}=-(\overline{u_i'u_j'}\frac{\partial u_j}{\partial x_k}+u_j'u_k'\frac{\partial u_i}{\partial x_k})-2\upsilon\overline{\frac{\partial u_i'}{\partial x_k}\frac{\partial u'j}{\partial x_k}}+\frac{p'}{\rho}(\overline{\frac{\partial u_i'}{\partial x_j}+\frac{\partial u'j}{\partial x_i}})+\frac{\partial}{\partial x_k}\left[\upsilon\frac{\partial u_i' u_j'}{\partial x_k}+\overline{u_i' u_j'u_k'}-\frac{p'}{\rho}(u_i'\delta_{ij}+u_j'\delta_{ik})\right]. \qquad (23)$$

By simplifying this equation, we have equations (24-25) as given below [26-27]:

$$\frac{\overline{Du_i'u_j'}}{Dt} = P_{ij} + \psi_{ij} - \varepsilon_{ij} + \phi_{ij} \text{ and} \tag{24}$$

$$P_{ij} = -(u_i'u_j' \frac{\partial u_j}{\partial x_k} + u_j'u_k' \frac{\partial u_i}{\partial x_k}), \tag{25}$$

which consists of 4 terms on RHS. These terms are Production, pressure strain, dissipation and finally diffusion.

For the turbulent flow in cyclones, the key to the success of CFD lies with the accurate description of the turbulent behavior of the flow [32]. To model the swirling turbulent flow in, there are different turbulence models available in Fluent. These range from the standard k-ε model to the more complicated Reynolds stress model (RSM) and large eddy simulation (LES) methodology, as an alternative for the RANS models. The standard k-ε, RNG k-ε and Realizable k-ε models are not optimized for strongly swirling flows found in cyclones or cyclonic flow regimes [31]. The RSM model requires the solution of transport equations for each of the Reynolds stress components and yields an accurate prediction on swirl pattern, axial velocity, tangential velocity and pressure drop on cyclonic flow regimes simulation [33].

LES has been widely accepted as a promising numerical tool for solving the large-scale unsteady behavior of complex turbulent flows. Encouraging results have been reported in recent literature and demonstrate the ability of LES to capture the swirling flow instability and the energy containing coherent motion of such highly swirling flows [34].

However, all methods will be used in this study except LES. The governing equations for LES and RSM can be found in the ANSYS Fluent user manual [35].

There are different approaches of mathematical (Analytical solutions) and also CFD (finite element solutions) for turbulent problems. Based on the fact that turbulent problems have perturbation and Reynolds Stresses terms, they need to be solved by more complicated state-of-the-art methods and programs to gain the best accurate reliable results.

The mathematical methods usually ignore various terms in Momentum (Navier-Stocks) equations to get them solved as simplified equations. The simplification process might solve the problem, but results could be far from reasonable and/or real condition.

K-Epsilon Standard is efficient only for high Reynolds numbers (Considering All nodes as turbulent flow passing). So, it is not appropriate to use this model for laminar low Reynolds numbers regions. Some geometries like Cyclones which have axial velocity almost zero near body walls also would get inaccurate results for some areas with this method.

The K-Epsilon RNG would be more efficient that K-Epsilon standard by using a mathematical equation called RNG, but it still gives some errors and negative values for several normal Reynolds stresses in particular condition. Thus, K-Epsilon realizable has been developed to cover these weaknesses.

For CFD solutions besides the famous time-averaging method, LES model is quite functional. This method, manipulating the Navier-Stocks (N-S) equations and defining new filters (Nodes bigger than mesh sizes), usually ignores small eddies with a reasonable outcome. Nowadays, using several simultaneous step-by-step methods for different stages of simulations are being carried out to get the most reliable results with less time consumed

4 Simulation

4.1 CFD (computational fluid dynamics):

Computational Fluid Dynamics (CFD) is a computer based mathematical modelling tool that can be considered the amalgamation of theory and experimentation in the field of fluid flow and heat transfer. It is now widely used and is acceptable as a valid engineering tool in industry. CFD calculations are based upon the fundamental governing equations of fluid dynamics: the conservation of mass, momentum and energy. These equations combine to form the Navier-Stokes equations, which are a set of partial differential equations that cannot be solved analytically except in a limited number of cases. However, an approximate solution can be obtained using a discretization method that approximates the partial differential equations by a set of algebraic equations. There are a variety of techniques that may be used to perform this discretization; the most often used are the finite volume method, the finite element method and the finite difference method. The resulting algebraic equations relate to small sub-volumes within the flow, at a finite number of discrete locations. A typical CFD simulation consists of several stages, described below:

A. Approximation of the geometry. The geometry of the physical system needs to be approximated by a geometric CAD type model. The more closely the model geometry represents the actual geometry, the more accurate the results are likely to be.

B. Creation of the numerical grid within the geometrical model. To identify the discrete, finite locations at which the variables are to be calculated, the geometry is divided into a finite number of cells that make up the numerical grid. Before doing this, it is

necessary to identify the physical flow phenomena expected (turbulence, compressible flow, shocks, combustion, multiphase flow, mixing, etc.) so the grid generated is suitable to capture these phenomena.

C. Selection of models and modelling parameters. Once the geometry and grid have been established, the mathematical models and parameters for those phenomena are then selected and boundary conditions defined throughout the domain.

D. Calculation of the variable values. Discretization yields a large number of algebraic equations (one set for each cell). These equations are then generally solved using an iterative method, starting with a first guess value for all variables and completing a computational cycle. Error or residual values are computed from the discretized equations and the calculations repeated many times, reducing the residual values, until a sufficiently converged solution is judged to have been reached.

E. Determination of a sufficiently converged solution. The final stage in the solution process is to determine when the solution has reached a sufficient level of convergence. When the sum of the residual values around the system becomes sufficiently small, the calculations are stopped and the solution is considered converged. A further check is that additional iterations produce negligible changes in the variable values.

F. Post Processing. Once a converged solution has been calculated, the results can be presented as numerical values or pictures, such as velocity vectors and contours of constant values (e.g. pressure or velocity).

G. Solution Verification and Validation Once the solution process is complete, each solution should be verified and validated. If this cannot be completed successfully,

re-simulation may be required, with different assumptions and / or improvements to the grid, models and boundary conditions used.

The computer has become a very valuable resource, and the continual increase in its performance gives great promises for the future. One of the areas that the computer has had a large impact in is fluid dynamics. Great progress has been made over the past several decades to incorporate computers into the prediction of fluid flow. The flow field around a complete aircraft configuration can now be calculated with the help of computers. The acronym CFD (computational fluid dynamics) represents numerical solutions to fluid problems by solving some form of the governing equations of fluid motion. Most complex engineering problems involve analysis from both CFD and experimental testing. The use of both of these approaches allows a more complete and detailed view of the flow field, enhancing the final solution. At the present growth rate of technology, research in both of these areas will continue to remain important and necessary in both the design and analysis of engineering problems. The complete Navier-Stokes (N-S) equations are considered to be the correct mathematical description of the governing equations of fluid motion. The most accurate numerical computations in fluid dynamics come from solving the Navier-Stokes equations. The equations represent the conservation of mass, momentum, and energy. In three dimensions, the conservation of momentum is written in each of the coordinate directions, giving a total of five equations to be solved. These equations are highly coupled and non-linear. Approximations to the Navier-Stokes equations are made whenever possible. For certain types of flows, these approximations can be made without compromising the physical modeling of the problem. Some of the various types of approximations will now be discussed. For laminar flows, solutions to the Navier-Stokes

equations are considered to be as accurate as numerical computations can be. But unfortunately, most problems where viscous effects are important are classified as turbulent flows. The unsteady Navier-Stokes equations have the ability to resolve all the small scale structure of turbulent flow. The problem is encountered with the enormous number of grid points required to capture all the physics of the flow. Therefore, it is more common to solve the Reynolds-Averaged Navier-Stokes (RANS) equations. These equations are the highest level of approximation. The equations solve for the mean flow field, which in turn requires a turbulence model for closure. In the world of CFD, there is no one turbulence model that is general enough for all flow conditions. Instead, each problem will need to be studied and have an appropriate model attached to it. In addition to a turbulence model, a relationship is required for the thermodynamic quantities. If a perfect gas is assumed, then the equation of state provides the necessary connection between thermodynamic variables such as density, pressure, and temperature. Some examples of where the RNS equations are applied are flow around a three dimensional obstacle [36], flow in an internal combustion engine [37], and unsteady oscillatory flow in an inlet [38]. The next level of approximation is to assume that the flow has a small amount of separation or backflow. For flows that are supersonic throughout the flow field (except for in the boundary layer), an approximation based upon the parabolic nature of the flow can made. All the information needed to advance the solution at a point is assumed to be along the upstream characteristic lines. The pressure field keeps the equations from being fully parabolic, so the pressure gradient must be suppressed to maintain the parabolic influence. Again the flow must be predominantly in one direction and supersonic. The equations for this level of approximation are called Parabolized Navier-Stokes (PNS) and

are discretized such that the solution is marched downstream [39]. PNS is not valid for separated flows in the streamwise direction, but can predict cross flow separation. Care must also be taken when shocks interact with the boundary layer since the interaction may separate the flow in the viscous shear layer. In general, the accuracy of PNS will be reduced as the Reynolds number is lowered. The next level of approximation depends on how the density varies throughout the flow field. If the density is compared to other flow parameters, such as pressure and velocity, then for most flows that occur naturally it could be stated that the variance in density is negligible compared to the other flow parameters. For example, the density of water is very close to being a constant over a large range of flow conditions. For air, the density can also be assumed constant without any significant loss of engineering accuracy for Mach numbers below 0.3. Because a large number of flows fall into this category, there exists an incompressible form of the Navier Stokes equations [40]. When density is assumed to be constant, the energy equation decouples from the mass and momentum equations, leaving one less equation to solve.

For three dimensional problems, the base number of equations to solve becomes four instead of five. Not only is it more efficient to solve the incompressible Navier Stokes equations at low speeds, but the compressible form of the equations become numerically stiff at low Mach numbers, which slow convergence considerably. When the Mach number drops below 0.1, the condition number of the RANS equations become very large due to the decoupling of the energy equation from the momentum and continuity equations. Under this condition, the solution quality will degrade as well. Getting away from the Navier-Stokes equations, the next level of approximation comes when the viscous layers are thin, allowing the separation of the viscous and inviscid parts of the flow. The viscous and

turbulent shear stresses must be confined to small regions close to the wall, making the pressure field predominately influenced by the inviscid nature of the flow. When the viscous terms in the Navier-Stokes equations are dropped, the result is the Euler equations. The Euler equations still require the solution of five equations for 3-D compressible flows, but the viscous terms no longer need to be computed. This results in a large increase in computational efficiency since the viscous terms no longer need to be computed and the computational grid does not need to be clustered near a wall to resolve the boundary layer. The Euler equations can be used to solve the inviscid flow field around a complete aircraft configuration. The next approximation under inviscid flows is the potential equation [41]. The potential equation is limited to irrotational flows. With the inviscid irrotational flow assumption, entropy will be constant over the whole flow field if the initial conditions reflect a state of uniform entropy. For a constant entropy flow, known as isentropic flow, a set of isentropic relations exist which become the basis for simplifying the Euler equations. This level of approximation may not seem very valid for many flows, but the fact is that the potential flow model is equivalent to the Euler equations for continuous, irrotational flows.

For subsonic flows around airfoils or wings, the solutions between the two should be almost identical. Only when shock waves become present are divergences in the pressure and velocity field seen. As long as the normal Mach number to a shock is less than 1.3, solutions are still comparable to the Euler equations. The single potential equation is an enormous reduction from the five equations associated with the Euler equations. Even though the potential equation is one of the lowest forms of approximation in fluid mechanics, it is still needed in engineering design and analysis. A large field of problems

exist for which potential flow solutions give valid results for a reduction in computational cost over other approximation levels. If a problem involves a slender or thin shape immersed in a flow that approaches the sonic condition, the transonic small-disturbance (TSD) equation can be applied. This equation is derived from the full potential equation, which does not assume any dominate flow direction. The TSD equation makes the assumption that the flow is predominately in one direction, with the flow in the normal direction being a small perturbation of the free stream flow. More information on TSD can be found in reference [42].

4.2 Model Design:

As discussed in previous sections, every CFD analysis must be associated with the physical most reliable model available. The reason is obvious; CFD, would cause probable errors either in numerical interpretation and/or in administrative input data inaccuracy or setting may not best suited for a particular problem to be solved. Thus, we have to make the most reliable physical model in CAD section of CFD, then try to impose all boundary conditions and grid meshes to describe the model in the best possible way. We have to look at the superconducting machines, both motors and generators, in order to reach our particular model problem needs to be simulated under special circumstances. So the next section follows, tries to depict the figures of this problem.

4.3 General structure of superconducting machines:

General and basic structure of a superconducting motor is shown in figure (9). Rotor, stator, windings and torque transfer components are the main parts of these systems.

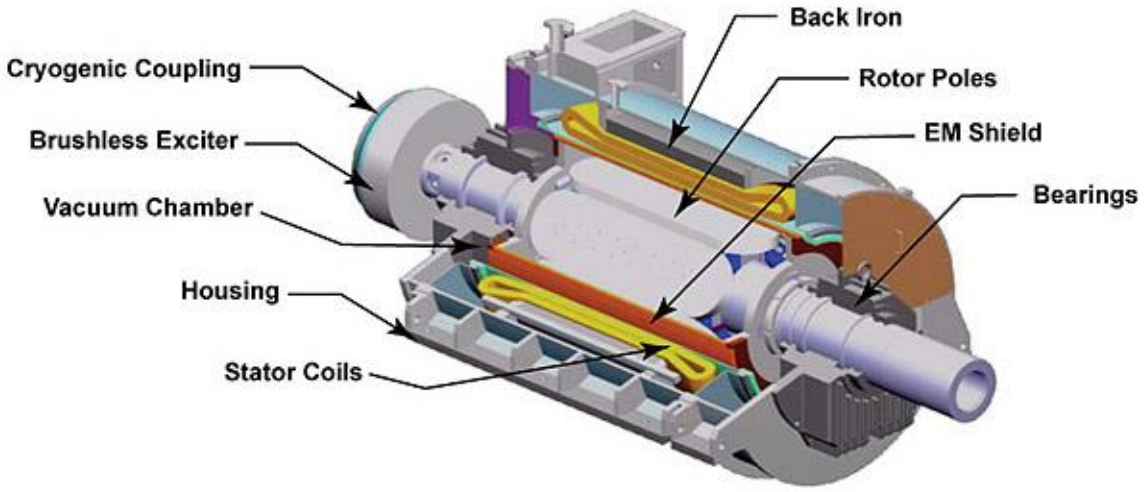

Figure 9.Conceptual cutaway view of a superconducting field machine (American Superconducting Co.)

After decades of planning and designing, real motors that use superconducting elements have been built and are now being tested by the U.S. Navy. American Superconductor Corporation and its partner Northrop Grumman [9]say they have completed successful full-power tests of a 36.5 MW (49,000 hp) high-temperature superconductor (HTS) ship propulsion motor at a naval site in Philadelphia. High Temperature Superconductor (HTS) material was first discovered in 1986. The resistance-free conductors are made of ceramic materials that exhibit superconducting properties at "high"

[9] Northrop Grumman is a leading global security company providing innovative systems, products and solutions in unmanned systems, cyber, C4ISR, and logistics and modernization to government and commercial customers worldwide.

temperatures between -250° and -150° C (In contrast to low temperature superconductors, which operate below -262° C. Both high and low temperature superconducting wire need to be cooled to cryogenic temperatures in order to exhibit the property of superconductivity, but HTS systems require less expensive cooling systems than low temperature superconductors. Liquid nitrogen at -200° C can be used for some HTS applications.

Details of the cooling system for the 36.5 MW motor were not revealed, but it is believed to be similar to a prototype 5 MW motor built and tested few years ago. The smaller motor is cooled with a refrigeration system that circulates helium gas in a closed loop to maintain the HTS field winding at cryogenic temperature. The performance of off-the-shelf cryocoolers has improved significantly in the past decade and have made HTS motors more feasible.

4.4 Successful tests

"The successful load test of our HTS motor marks the beginning of a new era in ship propulsion technology," said Dan McGahn, senior vice president and general manager of AMSC Superconductors.

"This motor provides the U.S. Navy with a truly transformational capability relative to size, stealth, endurance and survivability, providing our Navy with a clear performance advantage for years to come."

A typical naval destroyer will need two 36.5 MW engines for propulsion. Building such a motor with conventional technology results in an engine that is four to five times

heavier than an HTS motor. The HTS motor operates at 120 rpm and at a temperature of approximately 32K, which is -241°C. The cryogenic cooling system power consumption is less than a few percent of the total losses in the machine. Earlier last year, the Navy successfully installed an HTS degaussing coil onboard the USS Higgins. Powered by American Superconductor HTS wire and magnet cable technology, the coil system will undergo sea trials during the next two years. A comparison of a standard motor and a HTS motor is shown in figure (10).

Figure 10.Standard motor (rear) and HTS motor hugeness comparison

Degaussing coils, a vital part of today's military ships, are used to make military ships magnetically "invisible." They are used primarily a countermeasure to the threat of magnetic influenced mines. Since ships are mainly constructed of steel, they disturb the earth's natural magnetic field, which can be detected by sensors and weapons such as naval mines. Degaussing coils are composed of a network of electrical cables installed around the circumference of a ship's hull, running from bow to stern on both sides. Electrical current is passed through these cables to counteract the ship's inherent magnetic field,

controlled in such a way so that the ship is magnetically invisible. HTS technology can reduce the weight of the ship's degaussing system by up to 10 times that of a copper cable solution.

The U.S. Navy says it has invested more than $100 million in the development of HTS technology, paving the way not only for use in Navy ships but also in commercial vessels, such as cruise liners and liquefied natural gas (LNG) tankers.

HTS rotating machine technology is also being applied to the renewable energy industry. Wind generator systems utilizing HTS wire instead of copper wire are expected to be much smaller, lighter and more efficient than current systems. This will lower the cost of wind-generated electricity, particularly for offshore wind farms. Figure (11) shows schematic and real model of this machine.

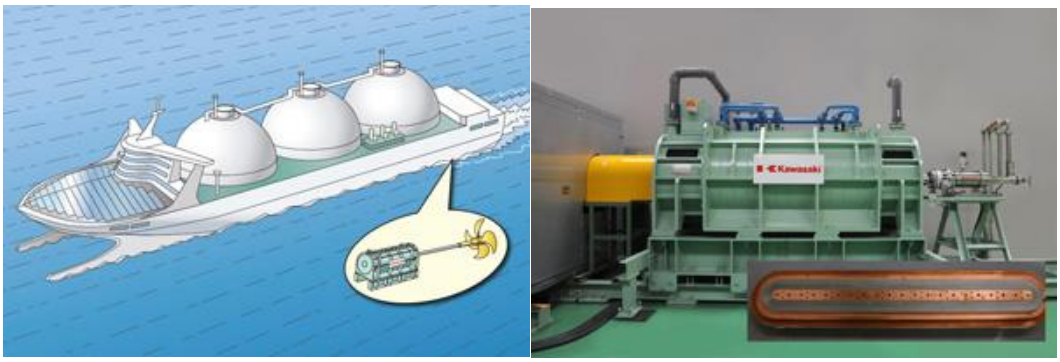

Figure 11.Superconducting motor prototype for ships

Tokyo, November 1, 2010 — Kawasaki Heavy Industries, Ltd. announced today that its prototype superconducting motor has broken a new record. The motor achieved Japan's highest power output of 450 kW in a test conducted at Kawasaki's Akashi Technical Institute in Akashi, Hyogo Prefecture. This achievement marks yet another

breakthrough in Kawasaki's research and development into space and energy-saving superconducting motors for large vessel propulsion systems as well as large-scale industrial drive systems.

4.5 NASA N3 turboelectric distributed propulsion Hybrid Wing Body aircraft (HWB) [43]

As already discussed in Introduction and literature review chapter, there are fundamental but differences between turboelectric and conventional aircrafts propulsion systems. This difference would be less between turboelectric distributed systems and hybrid ones. The HWB type aircraft presents an opportunity to reduce both fuel burn and aircraft noise.

Figure 12.N3-X Hybrid Wing Body (HWB) Aircraft with a turboelectric Distributed propulsion (TeDP)

For a quick imply on why this configuration was selected amongst all models, we can address these issues:

- The larger number of smaller fans allows more of the boundary layer to be ingested by low aspect ratio inlets while maintaining the thermal efficiency of a few larger core engines.
- The flexibility in distributing electrical power allows the number of power producing devices and the number of thrust producing devices to be independent of one another
- Distributing the power as direct current (DC) allows the speeds in the different devices to be independent of each other, essentially forming an infinitely variable ratio transmission between the power turbines and the fans
- Also electrical power from multiple devices can be readily mixed, allowing a degree of cross connection that is very difficult to achieve with mechanical power distribution

4.6 Model Description

The turboelectric distributed propulsion (TeDP) system illustrated in figure (12) consists of two turbo generators consisting of a turbo shaft engine driving superconducting electrical generator. The primary function of these devices is to make electricity, not thrust. The nozzle of the turbo generator is sized so that there is enough jet velocity at cruise to produce a small amount of net thrust to avoid being a source of drag; they are located on the wingtips so that the inlets ingest freestream air. Most of the energy of the gas stream is extracted by the power turbine to drive the generator. As a result the exhaust velocity is low which should result in low jet noise as well. The wingtip location will also give some bending moment relief in the normal direction at the cost of an increase in bump loading and possible aero elasticity considerations. There are other potential benefits of locating

the turbo generators on the wingtips [44] Research conducted in 1970 at NASA. Identified reductions in induced drag of up to 40% if a thrust producing device is located at the wing tip. The electric power from the turbo generators is distributed along redundant superconducting electrical cables to an array of superconducting motor driven fans in a continuous array of propulsors spanning the entire upper trailing edge of the center wing-body section .The width of the array is set to cover all of the long chord portions of the fuselage and wing root. This maximizes the amount of boundary layer ingested as measured by the swept area ahead of the propulsors with a minimum number of propulsors.

In fact, design of body, superconducting machines, electrical specifications and/or the placement of components are beyond the scope of this study and have been done by NASA and parallel Dr. Masson's research group works at university of Houston.

4.7 Electrical power system

We want to discuss the components required in a superconducting electrical power system supposed to be modeled for cooling system design. Similar work for these kind of analysis has been done already [45]. Two important materials used in this model is MgB_2[10] and BSCCO (bismuth strontium calcium copper oxide).

[10] **Magnesium diboride** (MgB_2) is a simple ionic binary compound that has proven to be an inexpensive and useful superconducting material.

4.8 Fully Superconducting Generator

Based on assumptions for this study, the required power density of motors and generators is obtained from wound rotor synchronous machines with superconducting windings on both rotor and stator. There has been some works on these sort of machines already done. [45] Figure (13) shows schematic drawing of a fully superconducting electric machine.

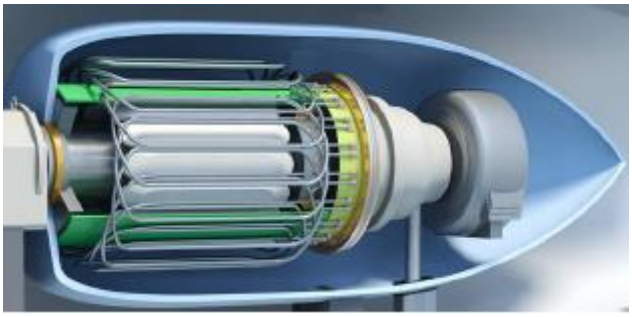

Figure 13.schematic drawing of a fully superconducting electric machine

The electrical components must operate under cryogenic temperature without any electrical leads between cryogenic temperature and room temperature. The windings in the stator of the generator are subject to alternating magnetic fields and alternating currents, AC. thus, AC losses would appear as waste of energy. These stator conductors must be designed carefully in order to reduce AC losses as much as possible. Also designing and optimizing the shape of conductors are beyond the scope of this study and can be referred to the works have already been done [46]. If MgB_2 is used to build turboelectric aircraft propulsion system, based on its intrinsic critical temperature which is 39K, the system must operate below 30K to provide the needed current density.so this must be of any cooling

system design consideration at first and most important step. Figure (14) shows a cross section view of this kind of design.

Figure 14.cross section view of MgB2 coils

Copper oxide (YBCO) concepts are kind of unsuitable for this design because of low advances have been done on these sort of materials to produce low AC loss.

4.9 Cooling System Design

Approaching the best design for heat exchanger, heat sinks and/or cooling systems, generally, calls for basic methods as Cryogenic system based on LH_2 or Reversed Turbo-Brayton cryocoolers. Also, the aim of simulation is to predict total cryogenic heat load and temperature distribution estimated using finite differences. The amount of cooling power needed is associated with the gradient between operation temperature (the source temperature) and the temperature at heat sink(heat being rejected at).the greater this difference ,the larger crycooler power required.in the next section follows immediately, we discuss why liquid hydrogen has been chosen as cry fluid.

4.10 Liquid Hydrogen (LH2) cooling

As discussed, although BSCCO material has a critical temperature above the boiling point of liquid nitrogen, the critical current density at liquid nitrogen temperature

is low to yield superconducting machines corresponding low weights in aerospace applications. This critical current density increases as temperature decreases. On the other hand, with a boiling point of around 20K at atmosphere pressure, liquid hydrogen provides an operating temperature that yields high current densities, which itself corresponds for smaller and lighter machines. We can also directly cool down MgB_2 with liquid hydrogen which has to operate under 30K.also using liquid hydrogen omits the greatest power loss in cryocoolers corresponds in the power transfer from turbines to the fans. This issue related back to transmission efficiency increase. Assumption of using liquid hydrogen is that hydrogen boils at constant temperature in the AC stator, so the hydrogen flow rate could be calculated.

4.11 Cryocoolers

As widely expressed and discussed in cryogenics chapter, the working mechanism of a cryocooler is exactly similar to conventional refrigerators. These systems need to be capable of keeping the TeDP systems temperature between 20K and 65K [47] .As what has been defined as efficiency, Carnot efficiency has the maximum theoretical value and all designs aim a portion of this value.

4.12 Modeling and simulation

Based on what has been depicted and explained, a cooling system must be modeled and simulated for both rotor and stator.as we know, an electric machine can operate as either a motor or a generator. The superconducting motors were sized with the same sizing code and treated in exactly the same fashion as the generators. Every simulation has five important parts as following:

- CAD design
- Meshing and grids
- Using a solver application as a finite element method
- Manipulating the results to get to best possible solution
- Validating the results using thermodynamics rules and/or comparing with experimental outcome

4.12.1 CAD design:

Modeling the geometry of problem is significant not only because of similarity to the major prototype, but also because of accuracy in meshing tools calling simple model to be meshed. Far beyond, every model must simplified by either dividing into some minor parts or by acceptable assumptions. The notion of this sentence is that a model must be designed which represents the whole idea of the prototype, and also reduces the time to be meshed, solved, verified and even more compared by other results, if possible. Therefore, we have to include the schematic 2D figure of our machine and then try to use simple, yet most effective CAD tools for modeling. Figure (15) shows the schematic of our machine.

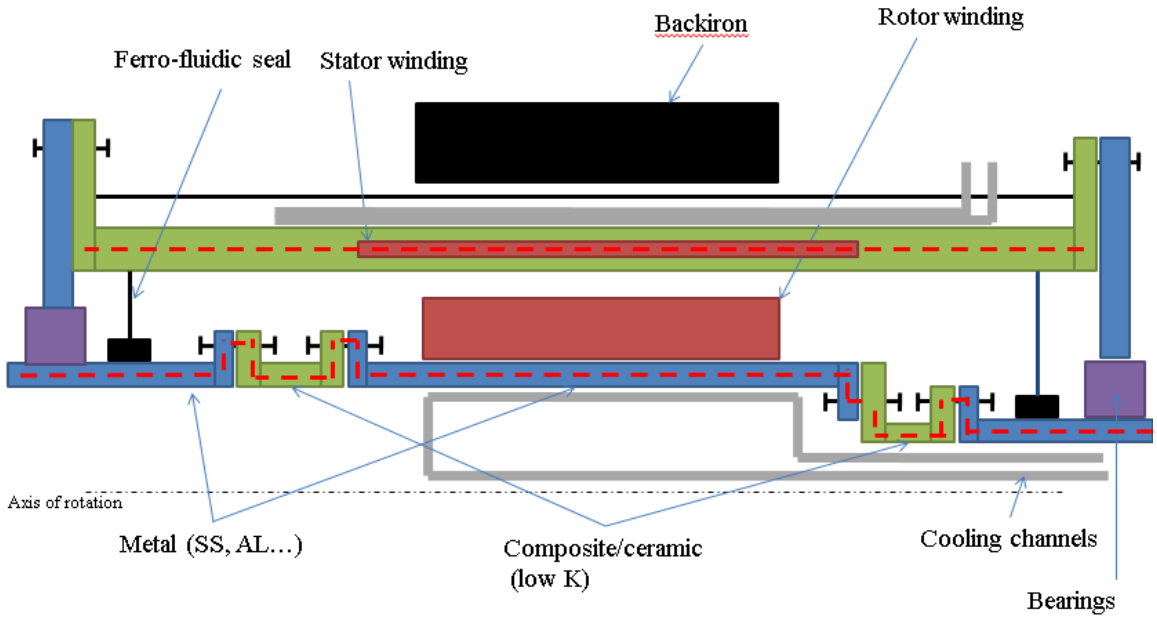

Figure 15.schematic diagram of machine used in this study

This schematic model for our particular machine consists of different components as followings:

- Shaft and bearings
- Rotor conductors and base
- Stator winding
- Cooling channels/pipes
- Cryostat wall and back iron
- Composite material like G10 as insulator
- Any additional materials like ceramics

All concepts of dimension calculations and/or assumptions have already been done by Dr. Masson's research group at university of Houston, and we only use the available dimensions to model our geometry.

There are different tools and applications to model a geometry such as CATIA, Solidworks, rhinhores, Rhinoceros 3D, AutoCAD. Choosing any of them must be considered based upon administrator ability and also the compatibility with meshing and solver application. Solidworks is used to model the graphical main model and CATIA has been employed to model the rotor and stator including cooling channels. Figure (16) shows the CAD model:

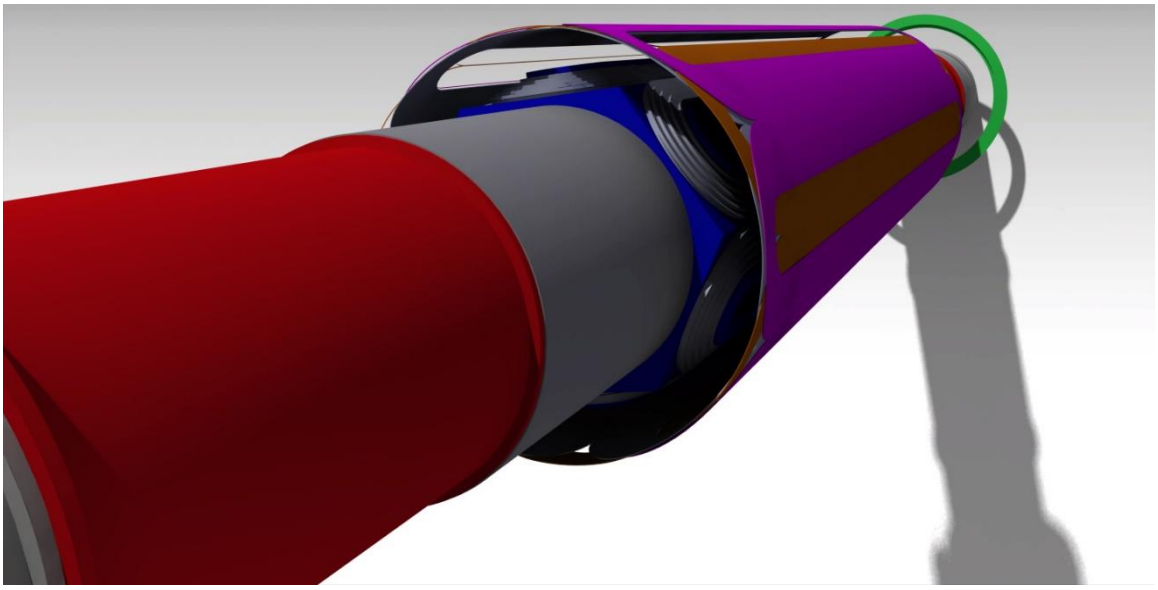

Figure 16.the CAD model

This figure shows the up view of this machine including shaft, stator winding, and rotor conductors. This model was configured and rendered again in CATIA V5R19.

4.12.1.1 Modeling cooling system:

As already covered in previous chapters and sections, cooling system must be designed particularly for two important elements shown in figure (17) in our superconducting machine: 1) rotor and 2) stator. We will discuss the works and ideas behind designing heat sinks and/or cooling channels for these two items separately. Figure (17) shows the rotor and stator windings.

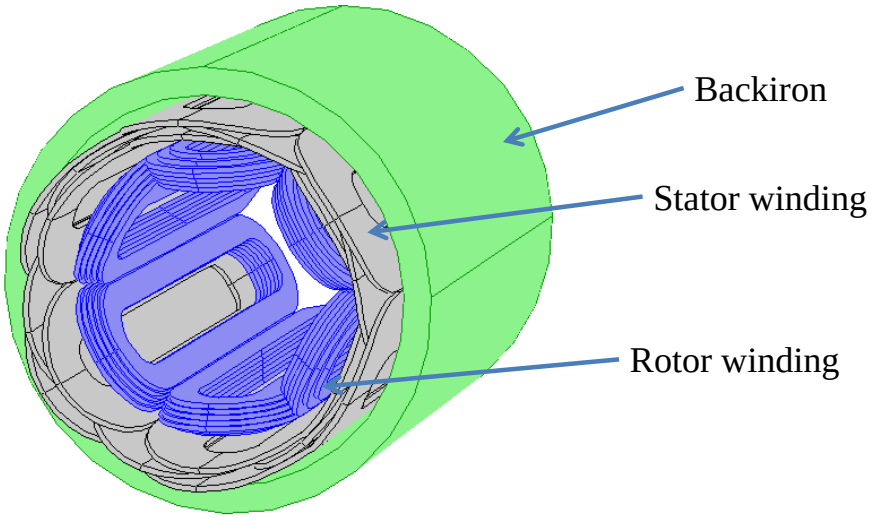

Figure 17.rotor and stator windings

Also, two schematic cross section views of our superconducting machine are depicted in figure (18), which also show the thickness of each element (walls, winding, conductors, rotor support, etc.)

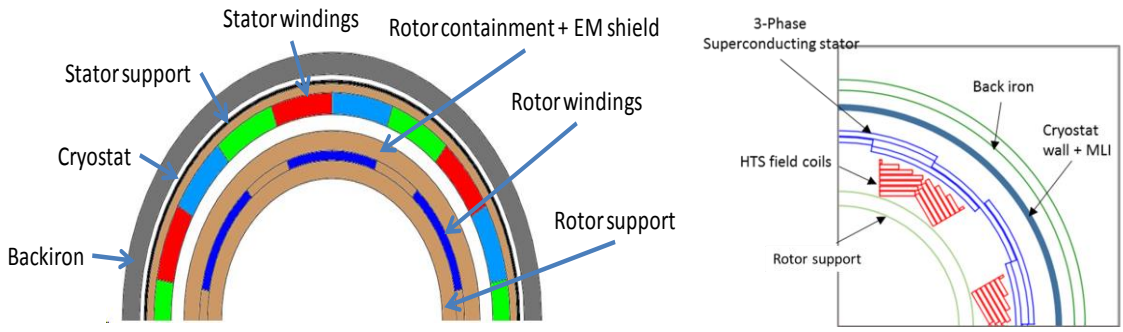

Figure 18.cross section views of our superconducting machine

4.12.1.1.1 Rotor cooling system:

Figure (19) shows the general dimension obtained by (research group in previous works) and for this study, only results have been employed for modeling.

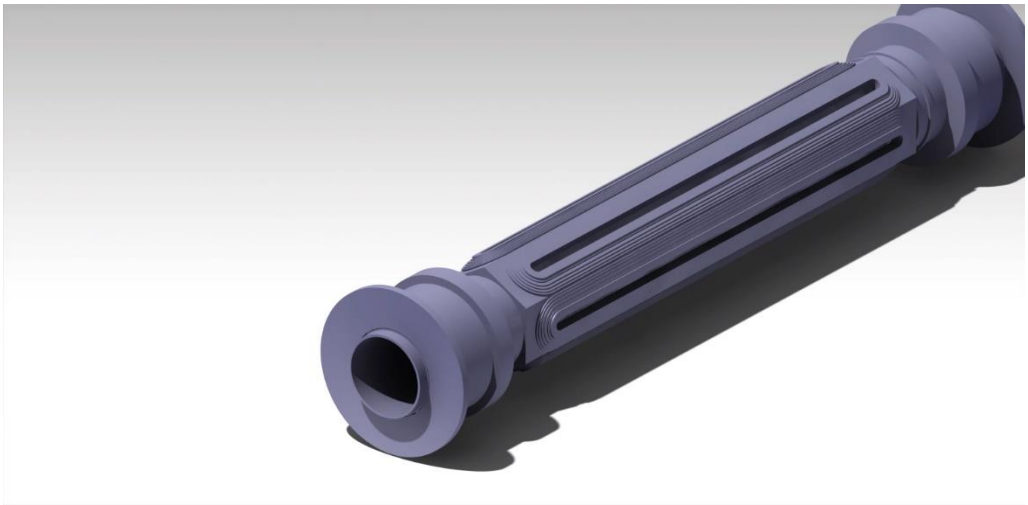

Figure 19.CAD model of our design

Two different proposed materials for shaft are steel and aluminum. Aluminum has been chosen for modeling and there are various cooling system designs that might seem of a

consideration value for every individual designer and engineer, yet in this two basic models will be proposed after different sketches tried as following:

- The channels going through racetrack support or base in meander shape
- The box of heat exchanger embedded in the shaft

4.12.1.1.1.1 The channels going through racetrack support/ base in meander shape configuration

Once a design is going through a designer mind, it doesn't seem that would perfectly match the whole idea of an effective sketch.nonetheless, it could lead us to try different configurations and opt the best model describing our geometry in as the best option based on time devoted to that specific work. This study is not an exclusion to that general rule or idea which is mentioned above. So, after various tries and efforts addressing and presenting different configurations, a more reliable, moreover, simple one would be selected amongst all.

The rotor schematic model design which is depicted in figure (20), shows that there are 6 racetrack included as well as their winding support. The material for both shaft and support is aluminum; one design would be a meander-shaped pipes or channels going through the whole racetrack support. However, if this design is selected, it means that conduction and convection both coupled together are responsible for cooling down the system. Liquid hydrogen is flowing through the channels and will cool down the support by convection. Similarly, this cold winding support would play a vital role to cool down the winding by conduction, since it is connected and fitted to racetrack winding.

For such this design, aluminum was opted for the material of channels and/or pipes. Figure (20) shows the simplified CAD model of rotor including shaft, support and channels embedded in the main body. The reason underlying why six half-circle channels are extruded out of main body is the low thickness of hexagonal shape of support. This design, preventing the intersection of channels walls to either shaft surface or upper wall of support connecting to winding. Figure (20) shows this CAD model:

Figure 20.CAD model of rotor cooling system and cooling channels going through support

The diameter of pipes would be a parameter of design and has to be verified and compared together in different analysis.

4.13 Meshing and simulation

The CAD model of our design can be directly imported to meshing tools. There are different methods to deal with this, yet importing under *igs* or *stp* file extension have some substantial benefits. Importing geometries including different components or

compartments would entail layers and surfaces to be considered. Thus, these extension might make the act of import free of confusion in parts naming and also the probable errors caused by unknown factors due to artificial intelligence deficiency of modeling softwares.in this study, ANSYS v15 tools have been deployed to mesh the model and solve the problem by numerical solutions.

Figure (21) depicts the meshes created by ANSYS mesh tools for this particular model.

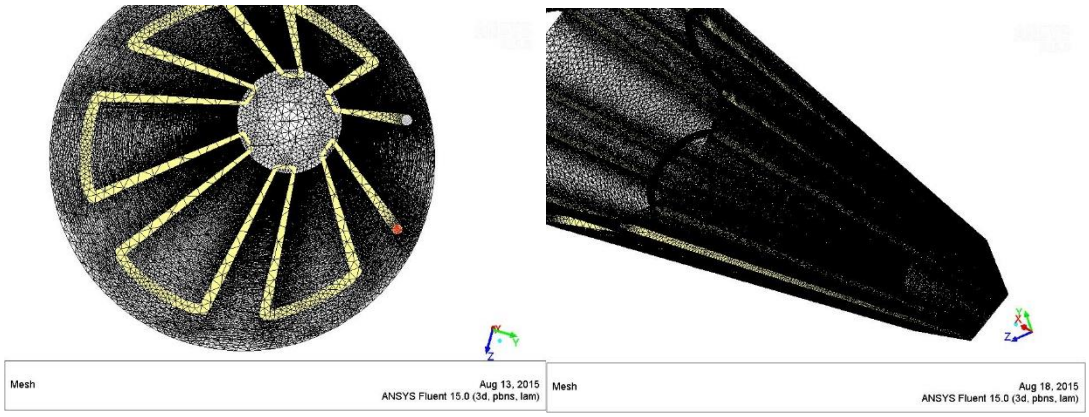

Figure 21.meshes created by ANSYS mesh tools for rotor cooling system

Having meshes created, the model must be imported to ANSYS Fluent for further numerical solutions as the last step.in Fluent, we have to deal the material, numerical method, initial and boundary conditions for geometry and fluid. Choosing these parameters would be the basic difference of each CFD try and might cause great perturbation in results by even negligible changes. Based on this fact, CFD methods and numerical solutions would be make indispensable changes case by case. Nonetheless, the K-e RNG method is

used to solve this problem. The differences of these mathematical solutions have been widely discussed in chapter 3.

4.14 Results

Figures (22) and (23) Show the temperature and pressure distribution in our model. Note that pressure distribution is only presented in pipes due to zero value in other solid components.

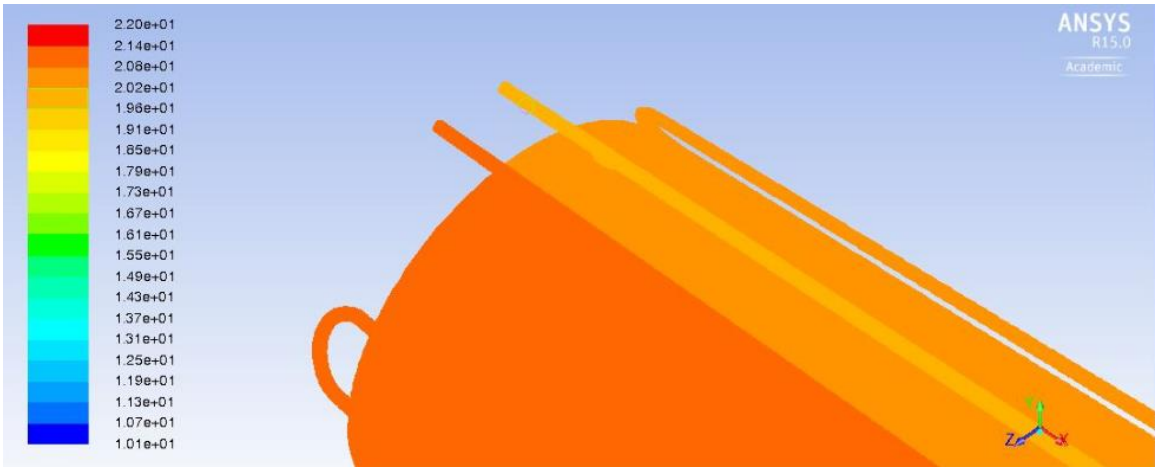

Figure 22.temperature distribution in a section including inlet and outlet of pipes

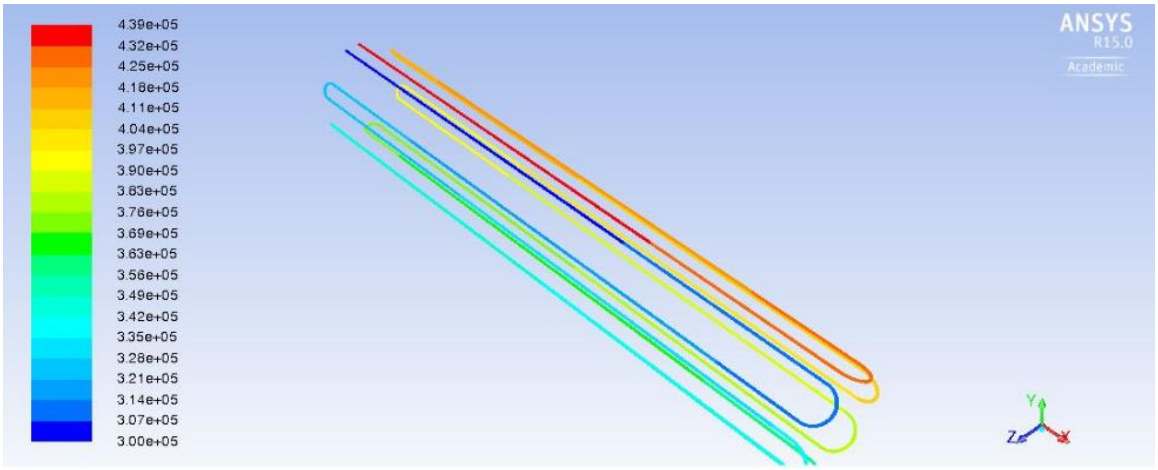

Figure 23.pressure distribution in pipes

Figures (24) and (25) plotted the temperature and pressure points all along the length of cylindrical shape of model.

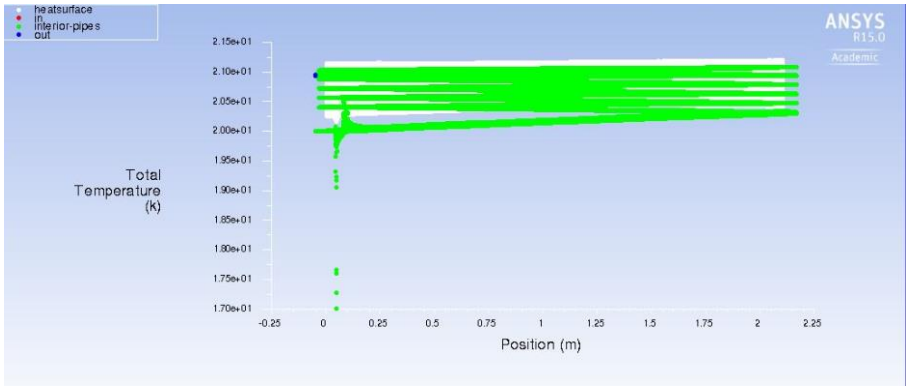

Figure 24.total temperature points plot

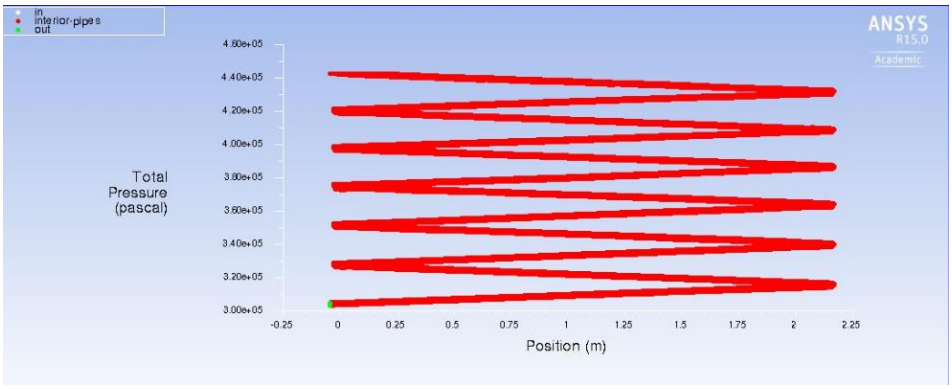

Figure 25.pressure points plot for fluid flowing in pipes

4.14.1.1.1 Stator cooling system

Similar to what has been carried out to make the simulation of rotor cooling system, the stator winding cooling system might benefit from liquid hydrogen high heat capacity and get cooled by coupled conduction and convection. The basic difference varies these two cases are:

- Amount of heat load must be rejected and dissipated to heat sink
- Non-rotational movement
- Lower thickness of windings
- Interdict of using metal materials for channels/pipes container and or surroundings

All these variations might seem negligible at first glance, yet it makes fundamental challenges in designing and results validations. Even though both cooling system ideas using liquid hydrogen as the coolant fluid, the more heat load in stator windings calls deeper considerations in shape of pipes, and also materials may avail as conductor surroundings.as we know, metals could not be used around the conductors in stator structure due to the induced current produced and affect the magnetic field in a negative way. However, approaching to the best idea to design cooling system in this study is based on using aluminum. The reason underlying this paradox is not complicated, relating to ease of use of aluminum as the basic conductive material in ANSYS Fluent. Once, an ideal configuration is found out for the cooling system, we could change the material and simulate the problem again to realize if the particular configuration could still provide efficient cooling performance. If the validation of result were positive and reliable, we could propose the configuration and discuss more concepts of using them based upon pros and cons. Another reason implying using a metal like aluminum for the first step of simulation, would be associated with its neutral effect of intrinsic thermal properties with magnetic specification. That is to say, when a thermal model went just under thermal and flow simulations, the effect of its magnetic effect and induced current would be

disregarded. Nevertheless, the writer will pass this method to readers as an individual approach might not seem vain for some individuals.

As mentioned above, conduction and convection integrative and uniting together, would be used as cooling system design for stator components. Figure (26) shows how stator winding located and conformed according to theory and design.

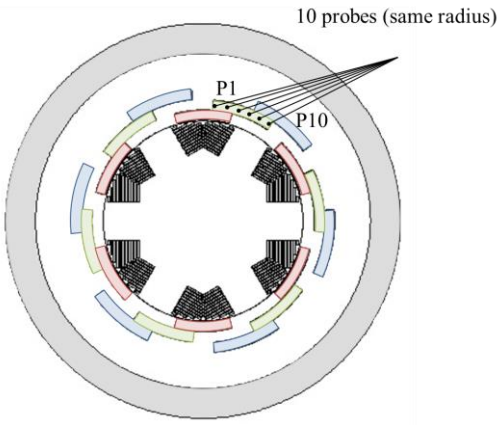

Figure 26.stator windings integration

One significant assumption for the following design is to expose all the heat load produced in conductors to the far top surface. Having this in mind, we could simplify our boundary conditions in an effective, yet reasonable way. In addition to that, assumption could reduce the numerical errors and perturbations which would be confusing and inaccurate, regardless to what challenges might be a head of us in meshing complex layers of winding.so like to previous work carried out for rotor, the stator cooling system CAD model has been created in CATIA V5R19.having disparate configurations simulated, a final design as opposite helical pipes including liquid hydrogen flow is proposed. The reason implying why two sets of channels used, is the great amount of heat load must be

rejected to heat exchanger around 4000W compared to 200W in rotor winding. The model is shown in figure (27):

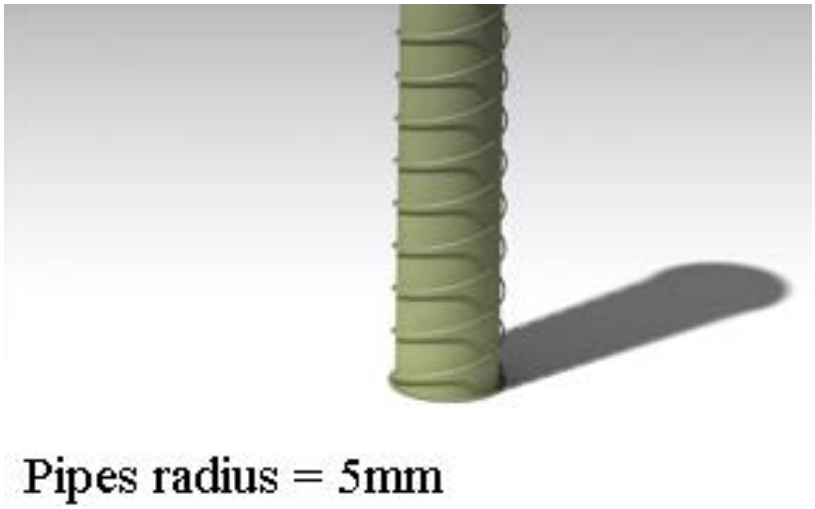

Figure 27.CAD model of stator cooling system showing opposite helical cooling pipes

Similar to simulation for rotor, turbulent k-e RNG model has been selected considering that flow is not laminar due to high Reynolds number. Stator winding is embedded in a composite material like G10 due to its mechanical and thermal properties which is shown in figure (27). However, regarding its low thermal conductivity, we are not able to use the whole channels container made from G10. The results of these simulation are brought in table (10) shows discrepancy in expectation and actual favorable outcome. Liquid hydrogen is flowing through a closed loop, gaining a high sufficient pressure by pumps with two inlets coming in an opposite direction in a helical form.in this phase, convection plays the active role to cool down the adjacent body which is of our interest to be selected amongst all material. Thereafter, in the second phase this body block which is cooled down takes the charge to absorb the heat from stator winding under conduction. The

more the heat capacity of fluid, the greater the amount of heat dissipated from conductor is. Far and beyond, opting for a material is a challenge must be resulting in good 1) thermal conductance and 2) mechanical strength. Figure (28) shows the cooling intermediate medium (block including LH2 pipes) of our design around stator.

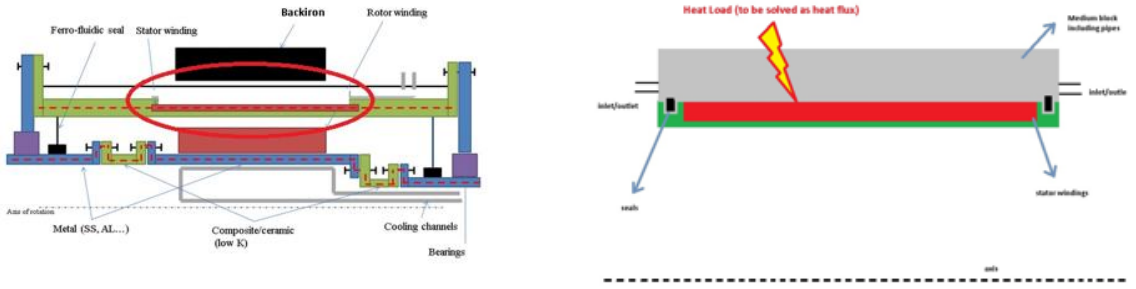

Figure 28. Schematic model for Stator heat exchanger block including LH2 pipes

4.15 Applying various materials

Obviously based on our previous discussions, aluminum could not be used in any component around stator in final model not because of having low thermal conductivity or heat capacity, but due to induced current and negative magnetic influence. Thus, other alternative materials ought to be compared and ranked based on these parameters:

- Reachability
- Cost
- Ease of implementation in the system
- High thermal conductivity and heat capacity

The results are summed up in the following section all together.

4.16 Results:

In this section, the results of simulation is given for aluminum as the material surrounding the liquid hydrogen channels at first step as fully explained above. Thereafter, the results of the rest of materials for the same geometry mark the highlights and differences. Changing heat flux initial value, velocity input magnitude of flow and diameter of the pipe would be the most necessary changes to find out the effect of manipulation geometry for a definite configuration.

For a constant heat flux value of 1000W/m2, the total temperature distribution are shown in figure (29) as input velocity of pipes changes from 6m/s to 12 m/s.

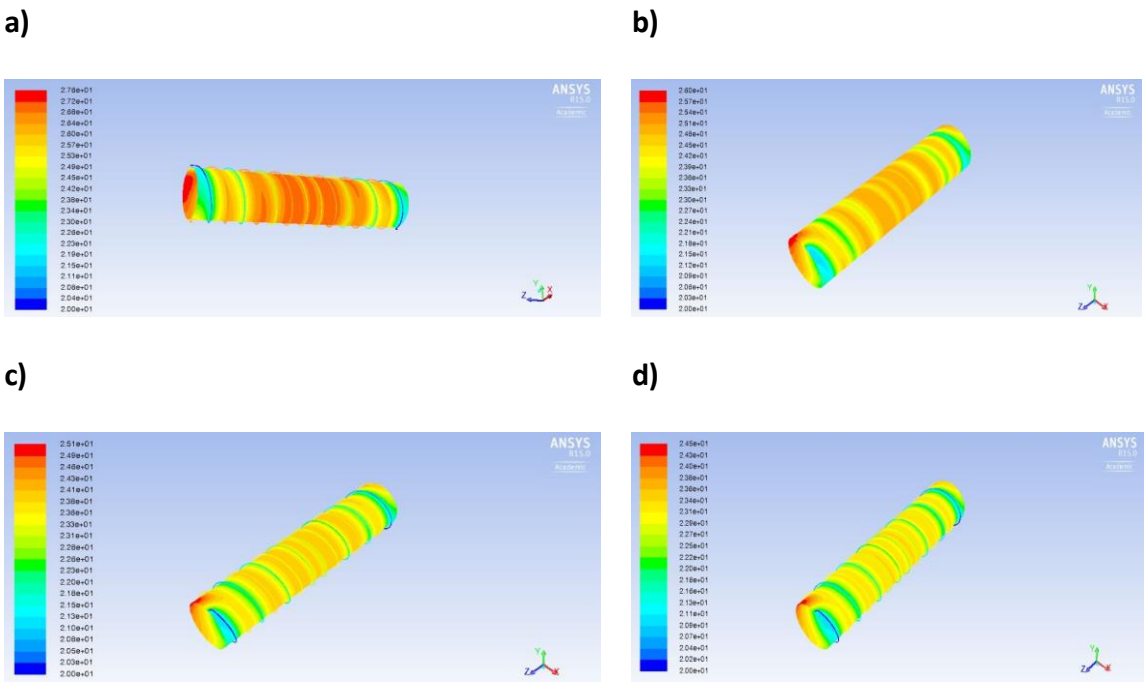

Figure 29.total temperature distribution for a) 6, b) 8, c) 10 and d) 12 m/s input velocity of LH2.

Similar act would be comparing the total temperature plots for exposed heat surface(the far top layer of stator winding) for two 6m/s and 8m/s inlet velocity magnitudes in a block together, to visualize and highlight the differences. Figure (30):

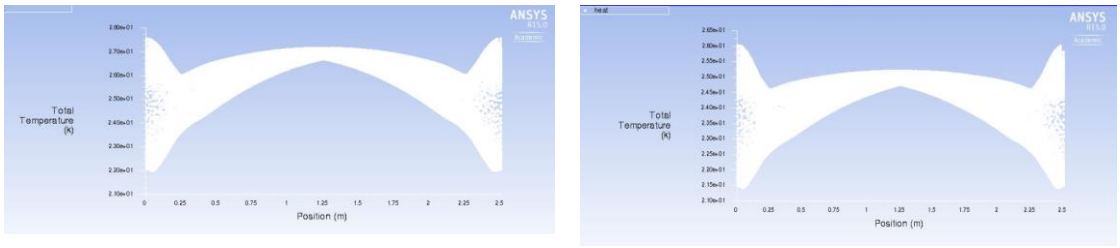

Figure 30.total temperature plot for two input velocities, 6m/s at left picture, and 8m/s at right one

Pressure gradient for liquid hydrogen in both helical pipes is of review interest. The reason is the thermodynamic properties and phase mode of fluid at pipes output. The design must consider the limitation to make the flow keeping only one phase not changing to gas throughout the pipes. If this occurs, there would be two-phase flow consists of liquid and gas, which is totally unfavorable.

Figure (31) shows the static pressure plots distribution as the input velocity changes from 6m/s to 8m/s(increment is 2m/s), at a constant heat flux of 1000w/m2 and assigned 5mm radius for pipes.

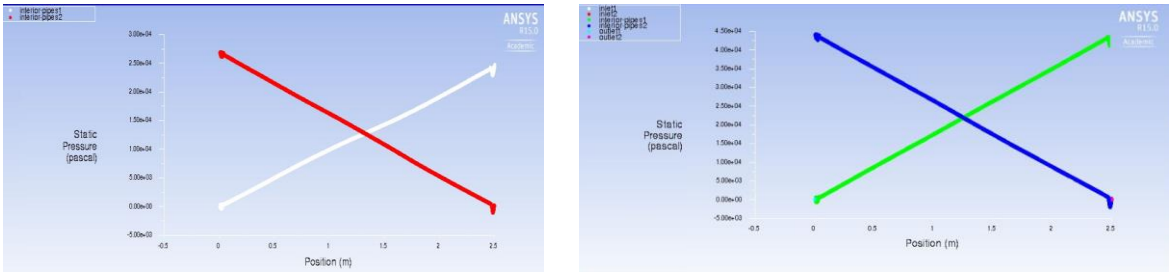

Figure 31.static pressure gradient plot for two input velocities, 6m/s at left picture, and 8m/s at right one.

Likewise what has been presented, tables (6-7) Show the values for maximum temperature as the most important design parameter in our study for two magnitude of heat fluxes (1000w/m2 and 1500w/m2).

Table 6.maximum temperature (K) obtained after simulation for 1000w/m2 heat flux

velocity / pipes radius	6m/s	8m/s	10m/s	12m/s
5mm	27.55178	26.02695	25.10659	24.48923
6mm	25.72467	24.67255	24.00527	23.57207

Table 7.maximum temperature (K) obtained after simulation for 1500w/m2 heat flux

velocity / pipes radius	6m/s	8m/s	10m/s	12m/s
5mm	31.32768	N/A	N/A	N/A
6mm	28.587	26.97915	26.0079	25.35811

The discussions on how and why these outcome are varied will be presented at conclusion sections. Based upon the technical prohibition (induced current) of using metals in stator surrounding, which already mentioned, other proposed materials like ceramics have undergone simulation for 1500W/m^2 exposed heat flux surface, and the results are gathered in table (9). But first, let's compare some novel materials properties to find the best candidates as the intermediate medium body. A good non-metal candidate must have:

- High thermal conductivity
- Lowest possible thermal expansion ratio
- High quality (pure)
- Lowest possible weight
- Reasonable cost (not to be exotic or expensive)
- Light weight

Meanwhile, based on researches have been done already on this hot issue, it could be stated that particular carbon or graphite foams are of the above mentioned favorable values. Table (8) gives us an outlook on this area.

Table 8.comparison of metals and non-metal carbon structured materials

Material	**Density g/cm3**	**Thermal conductivity (in-plane) W/m-K**	**Specific thermal conductivity (in-plane) W/m-K/(g/cm3)**
Copper	8.9	398	44.7
Aluminum	2.7	247	91.5
E-Glass/epoxy composite	2.1	0.16 to 0.26	0.1 to 0.2
Polymer composite	1.7	10 to 100	6 to 59
Natural graphite	1.94	370	190
Carbon foam	0.6 to 0.9	135 to 245	220 to 270
Ceramics	-	Low to high	-
ORNL Foam A	0.58	127	218
ORNL Foam B	0.56	175	313

As table (8) shows, copper and aluminum are brought as the most common high conductive metals. We can compare non-metals by these two ones. Also, ceramics and carbon foams like ORNL foams seems to be potential candidates for designing medium body of cooling system. Table (9) gives us a better vision on carbon-carbon composites and carbon foams thermal conductivity.

Table 9.some good carbon structured materials like carbon-carbon composites

Material	Thermal conductivity (in-plane) W/m-K
Single Wall Carbon nanotube	2000-6600
ORNL PocoFoam	285
BF Goodrich 3D	203
Pitch-Based Carbon Fiber(Discontinuous Fiber)	800
Pitch-Based Carbon Fiber(Continuous Fiber)	1100
POCO HTC	70(245 in-plane)
VGCF Carbon Fiber	1950

Based on evaluation of different materials already known, high thermal conductive ceramics like ALN (Aluminum Nitride) and particular graphite foams like ORNL foam would be of selection interest. Thus, similar simulation has been done for both mentioned materials (the procedure is exactly the same varying with substitution of aluminum in cooling block).the results of maximum temperature is given in table (10) for four different materials.

Table 10.maximum temperature (K) obtained after simulation for 1500w/m2 heat flux of proposed materials

Material	Maximum total temperature (K)
ORNL[11] graphite foam comparable to CVD Diamond	23.20581
G10	1400
Sapphire Polycrystalline(Al_2O_3)	23.251
Aluminum Nitride(ALN)	25
Quartz (Single Crystal)	23.08263

[11] Oak Ridge National Laboratory is the largest US Department of Energy science and energy laboratory, conducting basic and applied research to deliver transformative solutions to compelling problems in energy and security.

Figures (32) and (33) show the total temperature and pressure distribution plots, respectively, for graphite foam as a candidate and sample. We could obviously observe the temperature of LH_2 as liquid cryogen (coolant) will be maximum at center regions of magnets along the length of heat exchanger. This temperature rises sharply moving alongside over the heat flux surface (stator windings), reaching a peak, and then drops slightly when second inlet flow coming in the opposite direction (the same mechanism in popular heat exchangers).

a) **b)**

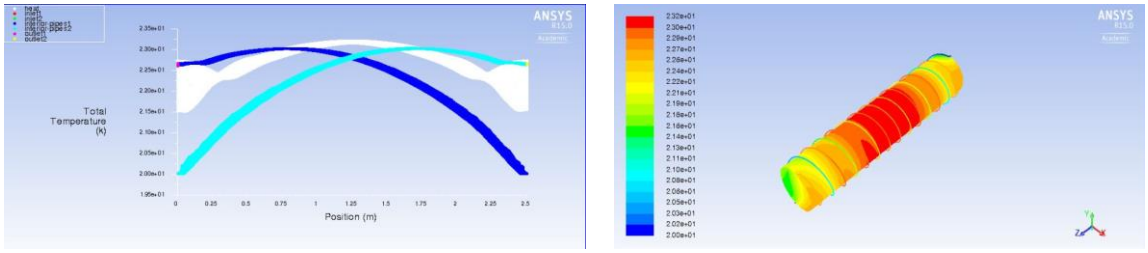

Figure 32. Total temperature distribution, a) plot and b) showing heat exchanger, for graphite foam comparable to CVD diamond.

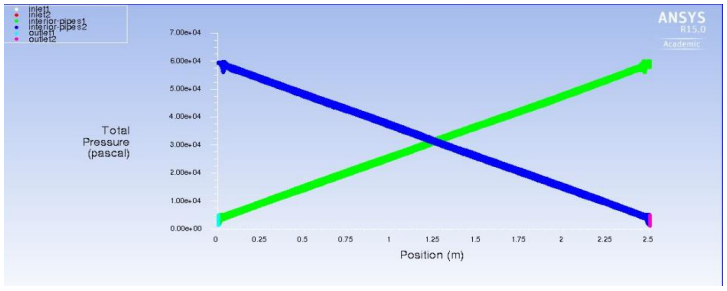

Figure 33. Total pressure distribution plot for Liquid Hydrogen alongside the length of stator heat exchanger for graphite foam comparable to CVD Diamond.

4.17 Challenges and future likely efforts

So far, we introduced two cooling systems for rotor and stator. Besides, we found out some unfavorable aspects of these sort of designs. Considering that no CFD work or simulation would be unique for any system, this study also could observe the problem in a fundamentally different way and obtaining results varied. Intrinsically, this is the main explanation why design and outcomes get improved and become even more precise with respect to time. Although, the results of this study is satisfactory and quite reasonable, some challenges might call for either future efforts or considerations. Two proposed concepts would be:

- Testing novel materials like new carbon or graphite structured foams
- Comparing the CFD results to experimental results and make a reasonable judgment
- Use other methods like direct cooling instead of indirect cooling(figure.34 shows a direct cooling method for stator hollow conductors)

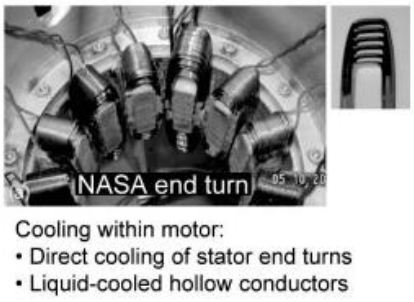

Figure 34. Direct cooling approach is shown for hollow conductors

5 Conclusions

Due to literature review in chapter (1), we realized the challenges of designing a fully superconducting machine, and also the major works which have been carried out so far. Basically, this study aimed to design a particular fully superconducting machine cooling system for both rotor and stator. We could sum up the conclusions as following:

- Aluminum could be used only as a common good thermal conductive material for testing different configurations of cooling systems only under CFD criteria. However, due to their induced current phenomenon, they must not be the final choice for any cooling system components around stator (this can be neglected for rotor).
- Meander-shaped pipes are employed for rotor cooling system under certain circumstances for this particular problem (final maximum temperature appeared in the system is in the acceptable range of design which is almost 20-30 K)
- Two opposite helical pipes for stator cooling system is proposed to cool down the stator windings. The pitch angle and pipes radius would be parameter of designs and may be varied model by model. Figure (35) shows the schematic 3D model of this heat exchanger. If the helical pitch angle of pipes is reduced, the pipes cooling area increases, however, the pressure gradient (pressure drop) would be of greater values. An optimal design must consider these aspects all together.
- Material are of great interest specially for designing stator cooling system, because there are different limitations in using metals which cause induced current

- Ceramics high conductive material like ALN(aluminum nitride), particular carbon-carbon composites and graphite(carbon) foams would be great candidates and alternatives for metal body of intermediate medium cooling system body
- The conduction and convection mechanisms coupled together are the main approaches of designing cooling systems in this study for both rotor and stator.
- The final phase of LH_2 would be of great interest. We must take special actions in our designs to keep that in liquid phase only. Fulfilling this aim refers us to pressure-temperature diagram of liquid hydrogen. As can be seen in figure (36), two regions for liquid (upper region), and gas (bottom region) are shown and divided by liquid-gas line. The lowest pressure of liquid hydrogen in heat exchanger pipes occurred at the outlet. Thus, with manipulation of outlet pressure value, by means of the outlet temperature, which the CFD results gives us, we could move the designing point to the liquid region. Therefore, special pumping systems are recommended providing sufficient kinetic energy to overcome the pressure gradient. The pumping system ability has a required minimum power value, however, the maximum design point would be more flexible depending on budget, space and maintenance. In this study, the lowest pressure occurs at outlet must be greater than 8bar for maximum favorable temperature which is 30 K.

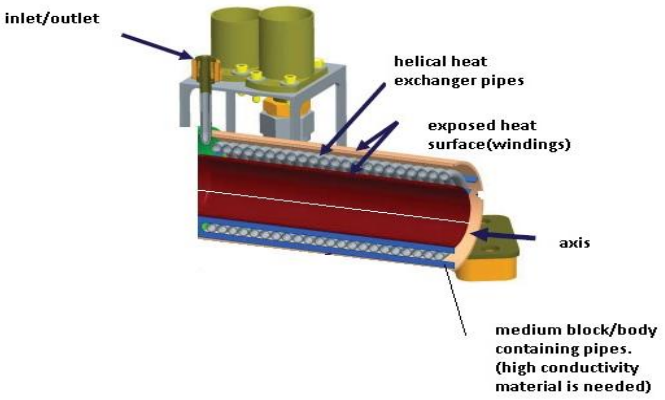

Figure 35. Schematic 3D model for heat exchanger

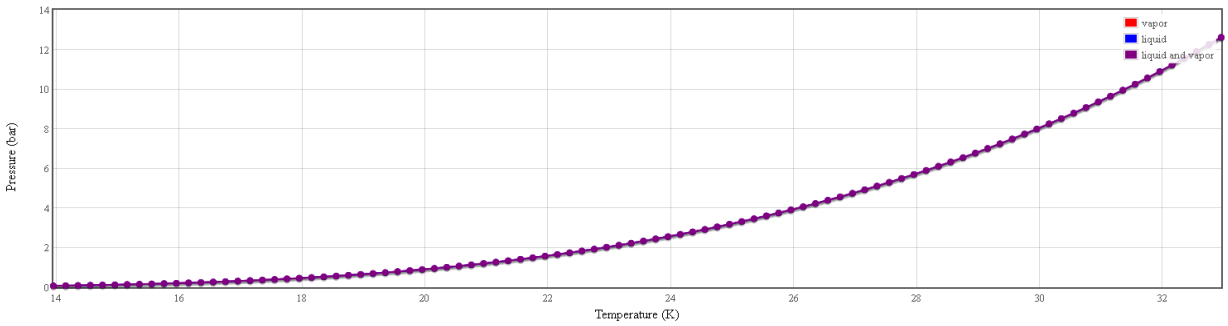

Figure 36.pressure-temperature (P-T) diagram for Liquid Hydrogen[12]

[12] Data from **NIST** Standard Reference Database 69: *NIST Chemistry Web Book, retrieved from http://www.nist.gov/srd/*

References

[1] Cesar A. Luongo, Senior Member, IEEE, Philippe J. Masson, Senior Member, IEEE, Taewoo Nam, Dimitri Mavris, Hyun D. Kim, Gerald V. Brown, Mark Waters, David Hall, "Next Generation More-Electric Aircraft: A Potential Application for HTS Superconductors." *IEEE Transaction and Applied Superconductivity* 19, No.3, Part 2,1055-1068 (2009)

[2] Amir S. Gohardani, "A synergistic glance at the prospects of distributed propulsion technology and the electric aircraft concept for future unmanned air vehicles and commercial/military aviation." *Progress in Aerospace Sciences* 57 (2013) 25–70

[3] Emadi, K &. Ehsani, M. (2000), "Aircraft power systems: technology, state of the art, and future trends." *IEEE Aerospace and Electronic Systems Magazine*, Vol. 15, (January 2000), pp. 28-32.

[4] Bradley, M., and Droney, C., "Subsonic Ultra Green Aircraft Research: Phase I Final Report." *NASA CR-216847*, 2011.

[5] Bruner, S., "NASA N+3 Subsonic Fixed Wing Silent Efficient Low-Emissions Commercial Transport (SELECT) Vehicle Study." *NASA CR-216798*, 2010.

[6] Meyer J. Benzakein, "What does the future bring? A look at technologies for commercial aircraft in the years 2035 – 2050."*Propulsion and Power Research* 2014;3(4):165–174

[7] W.R. Graham, C.A. Hall, M. Vera Morales, "The potential of future aircraft technology for noise and pollutant emissions reduction." *Transport Policy*, Volume 34, July 2014, Pages 36–51

[8] Gohardani AS, Doulgeris G, Singh R," Challenges of future aircraft propulsion: a review of distributed propulsion technology and its potential application for the all electric commercial aircraft." *Progress in Aerospace Sciences* 2011; 47(5):369–91, http://dx.doi.org/10.1016/j.paerosci.2010.09.001.

[9] Brown, Gerald V, "Efficient Flight-Weight Electric Systems." Presented at the Fifth Fundamental Aeronautics Program Technical Conference, Cleveland, OH, 2012.

[10] C.L. Tien, M.I. Flik, P.E. Phelan, "Mechanisms of local thermal stability in high-temperature superconductors." *Cryogenics*, 29 (1989), p. 602. [SD-008]

[11] J. G. Weisend. The Handbook of Cryogenic Engineering. Hardcover – July 1, 1998

[12] Meyer J. Benzakein,"What does the future bring? A look at technologies for commercial aircraft in the years 2035 – 2050." *Propulsion and Power Research* 2014;3(4):165–174

[13] H.J.M. ter Brake, and G.F.M. Wiegerinck, "Low-power cryocooler survey." *Cryogenics*, vol. 42, pp. 705-718, Nov. 2002

[14] James L. Felder, Gerald V. Brown, Hyun Dae Kim, "Turboelectric Distributed Propulsion in a Hybrid Wing Body Aircraft." NASA Glenn Research Center Cleveland, Ohio 44135 USA, ISABE-2011-1340

[15] Ogasawara, T, "Feasibility study on large-scale, high current density superconductor by dynamic stabilization, Part 1: magnetic stability. Part 2: stability margin." *Cryogenics* (1987) 27 673-681

[16] K Timmerhaus and T Flynn, Cryogenic Process Engineering. Plenum Press, NY (1989).

[17] Steward, W.G, "Transient helium heat transfer phase I – static coolant." *Int Journal of Heat Mass Trans* (1978) 21 863-874

[18] Lue, J.W., Miller, J.R. and Dresner, L. "Stability of cable-in-conduit Superconductors." *Journal of Appl Phys* (1980) 51 772-783

[19] P. K. GHOSHAL, "Cryogenics for high temperature superconductor (HTS) systems." Oxford Instruments NanoScience, Abingdon, UK

[20] S.K. Tyagi, S.C. Kuashik, R. Salhotra, "Ecological optimization of irreversible Stirling and Ericsson heat engine cycles." *J Phys D Appl Phys*, 35 (2002), pp. 2668–2675

[21] Frank P. Incropera ,David P. DeWitt ,Theodore L. Bergman,Adrienne S. Lavine, Fundamentals of Heat and Mass Transfer 6th Edition.

[22] https://simple.wikipedia.org/wiki/Heat_conduction.

[23] R P Reed and A F Clark, "Materials at Low Temperatures." American Society for Metals, Metals Park, Ohio (1983).

[24] The Goodall Chart, APT Division, UKAEA Culhum Laboratory, Abingdon, England (2009) (British Cryogenic Council, www.bcryo.org).

[25] J.Y. Chen, M.X. Shi, "Theoretical analysis on internal flow field of separation space in cyclone separators." *Journal of China University of Petroleum* 30 (6) (2006) 83–88.

[26] H. Safikhani, M. Akhavan-Behabadi, M. Shams, M.H. Rahimyan, "Numerical simulation of flow field in three types of standard cyclone separators." *Advanced Powder Technology* 21 (4) (2010) 435–442.

[27] B.E. Launder, G.J. Reece, W. Rodi, "Progress in the development of a Reynolds-stress turbulence closure." *Journal of Fluid Mechanics* 68 (3) (1975) 537–566.

[28] Y. Na, D.V. Papavassiliou, T.J. Hanratty, "Use of direct numerical simulation to study the effect of Prandtl number on temperature fields." *International Journal of Heat & Fluid Flow* 20 (3) (1999) 187–195.

[29] N.G. Deen, M.V.S. Annaland, M.A. Van Der Hoef, J.A.M. Kuipers, "Review of discrete particle modeling of fluidized beds." *Chemical Engineering Science* 62 (28) (2007) 44–50.

[30] J. Cui, X.L. Chen, X. Gong, G.S. Yu, "Numerical study of gas−solid flow in a radial-inlet structure cyclone separator." *Industrial and Engineering Chemistry Research* 49 (11) (2010) 5450–5460

[31] T. Chuah, J. Gimbun, T.S. Choong, "A CFD study on the effect of cone dimensions on sampling aerocyclones performance and hydrodynamics." *Powder Technology* 162 (2006) 126–132.

[32] W.D. Griffiths, F. Boysan, "Computational fluid dynamics (CFD) and empirical modelling of the performance of a number of cyclone samplers." *Journal of Aerosol Science* 27 (2) (1996) 281–304.

[33] M.D. Slack, R.O. Prasad, A. Bakkar, F. Boysan, "Advances in cyclone modelling using unstructured grids." *Transactions IChemE* 78 (2000) 1098–1104 (Part A).

[34] K.K.J.R. Dinesh, M.P. Kirkpatrick, "Study of jet precession, recirculation and vortex breakdown in turbulent swirling jets using LES." *Computers and Fluids* 38 (2009) 1232–1242

[35] ANSYS Fluent v.15, User's Manual, Accessed 2014.

[36] Rieger, H. and Jameson, A., "Solution of the Three-Dimensional Compressible Euler and Navier-Stokes equations by an implicit LU Scheme." AIAA Paper 88-0619, 1988.

[37] Schock, H. J., Sosoka, D. J., and Ramos, J. I., "Formation and Destruction of Vortices in a Motored Four-Stroke Piston-Cylinder Configuration." *AIAA Journal*, vol. 22, pp. 948{949, 1984.

[38] Newsome, R. W. J., "Numerical Simulation of Near-Critical and Unsteady Subcritical Inlet Flow Fields." AIAA Paper 83-0175, 1983.

[39] Hirsch, C., Numerical Computation of Internal and External Flows, Vol 2. John Wiley & Sons, 1990. ISBN 0-471-92452-0, pp. 70-72.

[40] Fletcher, C., Computational Techniques for Fluid Dynamics, Volume II. Springer-Verlag, 1991. ISBN 0-387-53601-9, pp. 26-33.

[41] Hirsch, C., Numerical Computation of Internal and External Flows, Vol 1. John

Wiley & Sons, 1988. ISBN 0-471-92385-0, pp. 108-127.

[42] Holst, T., Slooff, J., Yoshihara, H., and Ballhaus, W. J., "Applied Computational Transonic Aerodynamics." *AGARDograph* No. 266, 1982.

[43] Greitzer, Edward M, "N3 Aircraft Concept Designs and Trade Studies." NASA Contractor Report CR-2010-216794, Volume 1 and 2, , 2010

[44] Patterson, J.C., Flechner, S.G., "An Exploratory Wind-Tunnel Investigation of the Wake Effect of a Panel Tip-Mounted Fan-Jet Engine on the Lift-Induced Vortex." NASA TN D-5729, May, 1970

[45] Brown, G. V., "Weights and Efficiencies of Electric Components of a Turboelectric Aircraft Propulsion System", AIAA-2011-0225, presented at 49th AIAA Aerospace Sciences meeting in Orlando, FL, Jan 4-7, 2011

[46] Rindfleisch, M., "Low AC-Loss Magnesium Diboride Superconductors for Turbo-Electric Aircraft Propulsion Systems." NASA 2009 Phase 1, SBIR, NNX09CC75P, Hyper Tech Research, Inc.

[47] Diatez, A., "Thermal Management System for Superconducting Aircraft." NASA 2009 Phase 1 SBIR, NNX09CC77P, Creare Inc.